HELSINKI INSTITUTE OF PHYSICS INTERNAL REPORT SERIES

HIP-2019-07

Holographic Studies of Entanglement Measures

Arttu Pönni

Helsinki Institute of Physics
University of Helsinki
Finland

ACADEMIC DISSERTATION

To be presented, with the permission of the Faculty of Science of the University of Helsinki, for public criticism in the auditorium CK112 at Exactum, Pietari Kalmin katu 5, Helsinki, on the 12th of December 2019 at 14 o'clock.

Helsinki 2019

ISBN 978-951-51-5676-1 (print)
ISBN 978-951-51-5677-8 (pdf)
ISSN 1455-0563
http://ethesis.helsinki.fi
Unigrafia
Helsinki 2019

A. Pönni: Holographic Studies of Entanglement Measures,
University of Helsinki, 2019, 63 pages,
Helsinki Institute of Physics, Internal Report Series, HIP-2019-07,
ISBN 978-951-51-5676-1 (print),
ISBN 978-951-51-5677-8 (pdf),
ISSN 1455-0563.

Abstract

This thesis consists of four research papers and an introduction covering the most important concepts appearing in the papers. The papers deal with applications of gauge/gravity dualities in the study of various physical quantities and systems. Gauge/gravity dualities are equivalences between certain quantum field theories and classical theories of gravity. These dualities can be used as computational tools in a wide range of applications across different fields of physics, and as such they have garnered much attention in the last two decades. The great promise of these new tools is the ability to tackle difficult problems in strongly interacting quantum field theories by translating them to problems in classical gravity, where progress is much easier to make.

Quantum information theory studies the information contained in quantum systems. Entanglement is the fundamental property of quantum mechanics that sets it apart from classical theories of physics. Entanglement is commonly quantified by entanglement entropy, a quantity which is difficult to compute in interacting quantum field theories. Gauge/gravity dualities provide a practical way for computing the entanglement entropy via the Ryu-Takayanagi formula.

Entanglement of purification is an entanglement measure for mixed quantum states. It is in general a difficult quantity to compute in quantum field theories. Its proposed holographic dual, the entanglement wedge cross section (E_W), is however sufficiently simple to enable practical computation. We study the entanglement wedge cross section in various holographic backgrounds and entangling region shapes. We find systems where E_W exhibits nonmonotonous and noncontinuous behaviour. In particular, we study the ABJM theory coupled to massive fundamental matter and find nontrivial behaviour along the renormalization group flow between UV and IR fixed points.

We use holography to study different properties of quantum information in the ABJM theory with massive fundamental matter. We derive analytical expressions showing how the entanglement entropy and mutual information are affected by the introduction of fundamental matter. We introduce a new quantity called extensivity for characterizing the behaviour of mutual information under scaling of the entanglement region. The background represents a renormalization group flow between two fixed points. This interesting property of the background is studied by seeing how the mutual information, conditional mutual information and extensivity behave along the flow between the UV and the IR. Additionally, we calculate c-functions in order to measure the number of degrees of freedom at different length scales.

Noncommutative quantum field theories are interesting nonlocal theories with a minimal length

scale set by the nonvanishing commutator of spatial coordinates. We construct one such noncommutative theory by performing a series of string dualities on the known holographic background dual to the ABJM theory with massive fundamental matter. The string dualities produce a new gravity background which is interpreted to be dual to the noncommutative version of the initial theory. We study various quantities, including the Wilson loop, two-point function, and holographic entanglement entropy, focusing on their properties under changes in the amount of flavors or the length scale set by the noncommutativity.

The spherical black hole in global anti de-Sitter spacetime can be either stable or unstable depending on its radius. Small enough black holes are unstable and the thermodynamically stable phase in the canonical ensemble is thermal AdS. We compute the quasinormal modes and the spectral function dual to a massive bulk scalar field in the AdS-Schwarzschild background for different black hole radii, covering both the large and small black hole phases. We find that both quantities agree with their corresponding thermal AdS results when taken to the limit of small black hole radius.

Acknowledgements

First and foremost, I would like to thank my supervisors Niko Jokela and Aleksi Vuorinen for their guidance over the years. I have been fortunate to have so attentive supervisors available to help me whenever I needed it.

I want to express my gratitude to the pre-examiners, Giuseppe Policastro and Valentina Puletti, for giving me valuable comments on this thesis and Javier Mas, for agreeing to be my opponent. I also want to thank Vijay Balasubramanian, Yago Bea, Blaise Goutéraux, and Alfonso Ramallo for collaboration. Without your help, the papers on which this thesis is based surely would never have materialized.

I have received support for my PhD studies from the Magnus Ehrnroot Foundation and the Vilho, Yrjö and Kalle Väisälä Foundation of the Finnish Academy of Science and Letters. Additionally, the Doctoral Programme in Particle Physics and Universe Sciences has provided me with travel grants.

I would like to thank all of my training partners in Rebel Team / Delariva Finland and Karate Club Honbu. Regularly getting punched in the face and strangled is a surprisingly effective method for maintaining one's sanity through PhD studies.

Finally, I wish to thank my family and especially Elina for their continuous and essential support.

List of Included Papers

This thesis is based on the following publications [I, II, III, IV]:

I Notes on entanglement wedge cross sections

N. Jokela and A. Pönni

JHEP 1907 (2019) 87 1904.09582

II Information flows in strongly coupled ABJM theory

V. Balasubramanian, N. Jokela, A. Pönni, and A. Ramallo

JHEP 1901 (2019) 232 1811.09500

III Noncommutative massive unquenched ABJM

Y. Bea, N. Jokela, A. Pönni, and A. Ramallo

Int. J. Mod. Phys. A **33** (2018) no.14 1850078 (2018) 1712.03285

IV Small black holes in global AdS spacetime

N. Jokela, A. Pönni, and A. Vuorinen

Phys. Rev. D **93** (2016) no.8, 086004 (2016) 1508.00859

In all of the papers the authors are listed alphabetically according to particle physics convention.

The author's contribution

I The author did all of the calculations and produced all of the figures. The author wrote the article together with the co-author.

II The author did all of the calculations and produced all of the figures. The author also participated in writing the article.

III The author did the majority of the calculations and produced all of the figures. The author also participated in writing the article.

IV The author did all of the numerical calculations and participated in the analytical calculations. The author also participated in writing the article.

In addition to the included papers [I, II, III, IV], the author has an additional paper in which he performed most of the calculations and participated in the writing process [1]. Though related to the gauge/gravity correspondence, this paper was left out of this thesis in order to keep the subject matter more closely focused on holographic entanglement entropy and its applications.

Incoherent conductivity of holographic charge density waves

B. Goutéraux, N. Jokela, and A. Pönni

JHEP 1807 (2018) 4 1803.03089

Contents

Chapter 1

Introduction

One of the most influential discoveries in string theory in the last few decades is the *AdS/CFT correspondence*. The correspondence was discovered in the late 1990s and caused a wave of activity in subfields of theoretical physics continuing to this day. AdS/CFT provides a first principles based tool for studying quantum field theories (QFTs) in strongly interacting regimes, where traditional methods based on perturbation theory are deemed insufficient. While AdS/CFT does have its limitations, it has found success for example in predicting a lower bound for the ratio of the shear viscosity and entropy density in a wide class of quantum field theories in finite temperature [2].

The AdS/CFT correspondence is a holographic duality. It relates two seemingly unrelated physical systems to one another: a quantum field theory and a theory of quantum gravity in one higher spatial dimension. The first and best known example is the duality between a $(3+1)$-dimensional conformal field theory (CFT) and a type IIB superstring theory in a five-dimensional anti de-Sitter (AdS) spacetime times a five-dimensional internal sphere [3]. Since string theory is not yet very well understood, we need to work in a limit which makes the duality more practically useful. In the CFT we may consider the limit where the gauge group rank and coupling constant are large. It turns out that on the string theory side this limit corresponds to taking the string length and string coupling constant to be small, and thus the string theory is well approximated by classical gravity. In this limit, the duality is between classical gravity and a strongly interacting CFT, making it possible to perform calculations on the gravity side and translate them to results in the CFT. The reason for the string theory to simplify in this limit is that both quantum and stringy effects are suppressed. The shortness of the string length compared to the curvature radius of the AdS space causes the strings to look like point particles instead of extended objects, thus suppressing all but the massless string excitations. The smallness of the string coupling constant suppresses quantum effects of string loops and enables us to ignore the quantum fluctuations of the background spacetime. In other words, holographic dualities state that certain strongly interacting QFTs are such that their collective dynamics gives rise to emergent weakly coupled gravitational degrees of freedom.

It is a surprising discovery that two physical theories in different spacetime dimensions should be equivalent to each other. After all, it seems implausible for a lower dimensional theory to hold the same information content that a higher dimensional theory contains. In order to see that such a duality

could be possible, let us consider the number of degrees of freedom, as measured by entropy, on each side of the correspondence. Let the QFT under consideration live on a d-dimensional manifold. The entropy of some spatial region at constant time is extensive in the volume of that region. That is, the entropy is proportional to a $(d-1)$-dimensional volume. Now consider the dual gravity side which describes the dynamics of a $(d+1)$-dimensional manifold. Contrary to the naive expectation, the entropy of a spatial region at constant time is not proportional to the volume, but to the surface area of that region. This is a special property in gravitational theories: the entropy of a spatial volume is bounded by the entropy of a corresponding black hole. The entropy of a black hole is given by the Bekenstein-Hawking formula [4]

$$S_{BH} = \frac{A}{4G_N^{(d+1)}} \ , \tag{1.1}$$

where A is the area of the event horizon and $G_N^{(d+1)}$ is the gravitational constant in $(d+1)$ spacetime dimensions. In other words, the entropy of a spatial volume in a gravity theory is proportional to the boundary area of that surface which in our case means a $(d-1)$-dimensional volume. Thus, the entropy of the gravitational theory can indeed match the entropy of the QFT. This is all because the degrees of freedom in quantum gravity are organized in a way that information about a spatial region can be encoded on the boundary of that region [5, 6].

Since the original discovery of the AdS/CFT correspondence, many generalizations have been found, collectively known as *gauge/gravity dualities*. For example, generalizations have been found for theories in finite temperature and confining cases, in various dimensions. Dualities can be found by the so-called top-down approach where one starts in string theory and derives a duality. The other way is to work bottom-up, by directly writing down a gravity background which exhibits the physics one wants to study. The drawback of the former approach is the difficulty of finding string theory solutions. The drawback of the latter is the lack of knowledge about the dual QFT represented by the gravitational background.

The AdS/CFT correspondence has applications in multiple branches of theoretical physics. One important application is in the study of the dynamics of strongly coupled plasma, where difficult nonequilibrium dynamics are converted to feasible problems involving numerical solutions to Einstein's equations. Even though the plasma modelled by holographic calculations is usually supersymmetric and has a large number of colours, it still produces reasonable results when compared to real QCD plasma formed in heavy ion collisions. It seems that there is some universality in a wide class of strongly coupled QFTs which makes it possible to use holographic toy models for making qualitative predictions for real QCD plasma [7, 8]. An another avenue for applications is in condensed matter theory. Examples of applications of AdS/CFT in this context include superconductors [9] and strange metals [10].

Entanglement entropy is an important quantity in quantum information theory, but its calculation is prohibitively difficult in all but the simplest QFTs. Fortunately, the AdS/CFT correspondence equates the entanglement entropy of a QFT with the area of a certain surface in the gravity side [11]. The geometrization of entanglement entropy makes it a practical quantity to compute in interacting field

theories with gravity duals.

This introduction to the thesis is primarily concerned with the entanglement entropy and quantities derived from it, in the context of gauge/gravity dualities. We will cover other information theoretical quantities and concepts appearing in the included papers. In Chapter 2 we introduce the quantities from classical information theory which are most useful to us, after which we cover their quantum counterparts. In Chapter 3 we start by discussing the anti de-Sitter space and its most important properties. Then we introduce the holographic entanglement entropy and show examples as to its use. We also cover related quantities, such as the mutual information and entanglement of purification, along with their holographic realizations. In Chapter 4 we give concluding remarks.

Chapter 2

Quantum entanglement entropy

In the early days of quantum mechanics it was realized that the predictions of quantum mechanics cannot be described by a local hidden variable theory due to quantum entanglement. Quantum entanglement is a phenomenon in which two particles can behave as one in such a way that measurements on one will instantaneously affect measurements performed on the other [12]. Local hidden variable theories are attempts to describe quantum phenomena in a way that preserves locality while simultaneously avoiding the kinds of indeterminism that are present in quantum mechanics. These theories put forward the idea that there should exist some variables associated to particles which predetermine the results of all conceivable measurements independently of any observer. Quantum mechanics on the other hand is a fundamentally probabilistic theory. In quantum mechanics, the result of a measurement is not determined before the measurement is carried out. Some physicists found this objectionable, Albert Einstein famously being convinced that God does not play dice, and tried to find alternative models for quantum phenomena. It was shown that the statistical correlations that are possible in a hidden variable model obey the so-called Bell inequalities [13] which were later experimentally proven to be violated by nature, ruling out any local hidden variable descriptions of our world [14, 15].

Entanglement is the fundamental property that distinguishes quantum mechanics from classical theories of physics and its presence is thus responsible for many of the strange quantum properties of nature. Entanglement causes different parts of a system to behave as one in a fundamental way, even when the parts are not interacting with one another. Usual intuition is that one should be able to study the behaviour of the non-interacting parts separately and thus understand the behaviour of the full system. This intuition fails if the parts of the system are entangled, regardless of the parts not interacting with one another or even being separated by a vast distance. We will give simple examples that illustrate some of the surprising properties of quantum entanglement later in this thesis. Since entanglement is purely a quantum phenomenon, its presence can be seen to signal the quantumness of a given physical system. Different quantities have been developed for measuring the amount of entanglement in a given system. One of them is the entanglement entropy which is the quantity around which this thesis revolves.

We start this chapter by introducing the concept of entropy, a quantity which describes the amount

of uncertainty about a system, first in the context of classical information theory. We will also introduce multiple quantities closely related to entropy and discuss their properties. Lot of these classical information theory concepts have their quantum counterparts and it is instructive to compare the similarities and differences between classical and quantum quantities in order to gain some intuition about them. After covering the relevant concepts in the context of classical information theory, we turn to study quantum mechanics. We will quickly cover the relevant foundational features of quantum mechanics and then work our way towards entanglement entropy and related quantities.

2.1 Classical information theory

Entropy is a measure of uncertainty in a physical system. Much of information theory revolves around the concept of entropy. Entropy assigns a non-negative number for a physical system in such a way that higher entropy indicates higher uncertainty about the state of the system and vanishing entropy indicates that the state of the system is perfectly known. Framed in an another way, entropy characterizes the amount of information one gains by learning the state of the system. For example, in a binary system which can occupy one of two states, one with probability p and the other with probability $1-p$, entropy of the bit should be highest when $p = 1/2$ since in this case both states are equally likely. The entropy should vanish for $p = 0$ and $p = 1$ since in that case the state of the system is perfectly known.

Consider a discrete random variable X with N possible values and the associated probability distribution assigning numbers $0 \leq p(x) \leq 1$ for each realization $X = x$. The *Shannon entropy*, denoted by $H(X)$, of this probability distribution is defined as [16]

$$H(X) = -\sum_{x \in X} p(x) \log_2 p(x) = \langle -\log_2 p(x) \rangle \ , \tag{2.1}$$

where we have adopted the notation $\langle \cdot \rangle$ for the expectation value in anticipation of quantum mechanical treatment of entropy. The entropy (2.1) can be seen to be positive and vanish only for a distribution where one specific realization of X occurs with certainty[1]. Also it is easy to show that $H(X)$ is maximized when $p(x) = 1/N$, in which case $H(X) = \log_2 N$. All of these features is what we intuitively expect when entropy is supposed to quantify our uncertainty about the value of a random variable.

The Shannon entropy $H(X)$ expresses the average number of bits of information carried by a message comprised of letters drawn from the probability distribution of X. To see this, we return to the example of a binary random variable with $p(X = 0) := p$. A message of length n is a string of n letters drawn from the distribution of X. The key realization is that in order to store messages, one only needs to consider how many different typical messages there are. For long messages $n \to \infty$, on average, np of the letters are zeros and the rest are ones. The number of messages of this kind is

[1] As is conventional, by $0 \log_2 0$ we mean the limit $\lim_{x \to 0} x \log_2 x = 0$

$\binom{n}{np}$, which can be approximated in the limit of long messages by

$$\binom{n}{np} = 2^{\log_2 \binom{n}{np}} \approx 2^{n(-p\log_2 p-(1-p)\log_2(1-p))} = 2^{nH(X)} \ . \tag{2.2}$$

Now one can use a code in which each of these typical messages is represented by an integer. For a binary random variable, $0 \leq H(X) \leq 1$, we see that the number of typical messages (2.2) can be considerably lower than the number of all messages, 2^n, depending on p. For $n \to \infty$, the probability of a message being atypical is small. The same logic generalizes to the case where X is not binary. This was one of Shannon's [16] results: a message of length n contains, on average, $nH(X)$ bits of information instead of the naive expectation of n bits. Conversely, if one tries to code a n letter messages to fewer than $nH(X)$ bits, error rate in decoding would be large because this scheme would not be able to encode all frequently occurring messages.

The Shannon entropy works just as well for multiple random variables. For example, in the case of two random variables $X, Y \sim P(X, Y)$, the Shannon entropy is

$$H(X,Y) = -\sum_{x\in X, y\in Y} p(x,y)\log_2 p(x,y) \ , \tag{2.3}$$

and for more random variables the above formula extends in the obvious way. The entropy of a joint probability density has many interesting properties, including

1. $H(X) \leq H(X,Y)$: uncertainty about the joint system X, Y is never less than the uncertainty of one of its parts X. This inequality saturates either when Y is trivial or when X and Y are perfectly correlated, or in other words, knowing the value of X implies a definite value for Y.

2. For three random variables X, Y, Z the following always holds

$$H(X,Y,Z) + H(Z) \leq H(X,Z) + H(Y,Z) \ , \tag{2.4}$$

   with equality when X and Y are independent given Z. This property is called *strong subadditivity*.

3. In the special case when Z is trivial, the above reduces to

$$H(X,Y) \leq H(X) + H(Y) \ . \tag{2.5}$$

   This property is called *subadditivity*, and the inequality saturates when X and Y are independent random variables. Subadditivity states the intuitive fact that the uncertainty one has about a joint system never exceeds the sum of uncertainties one has about the parts of the system. This is as it should be, since if X and Y are correlated, measuring one gives at least some information about the other.

At this point we note that the first listed property implies $\max(H(X), H(Y)) \leq H(X,Y)$, an inequality which is spectacularly violated by the quantum extension of entropy explored in Section 2.2.

Now a sensible question to ask is how uncertain we are about X, if Y is known. Say we know the joint distribution $p(x, y)$ and have already observed that $Y = y$. Given this information, we know that $X \sim P(X|Y = y)$. The entropy of this distribution would still be a random variable over Y, whose expectation value is what we call *conditional entropy*, $H(X|Y)$

$$H(X|Y) = \langle H(X|Y = y)\rangle_Y \ . \tag{2.6}$$

This form shows explicitly that the conditional entropy quantifies the average residual uncertainty one has about the value of X once the value of Y has been observed. $H(X|Y)$ can be related to $H(X, Y)$ and $H(Y)$ by

$$H(X|Y) = H(X, Y) - H(Y) \tag{2.7}$$

which is conventionally taken as the definition of $H(X|Y)$. This definition clearly shows that $H(X|Y)$ measures the residual uncertainty about X after learning the value of Y, giving $H(Y)$ bits of information. The conditional entropy is unsurprisingly non-negative $H(X|Y) \geq 0$, with equality only when X has definite value given Y, thus leaving no uncertainty after one learns the value of Y.

The conditional entropy satisfies the following property

$$H(X|Y, Z) \leq H(X|Y) \ , \tag{2.8}$$

which follows from the definition of conditional entropy (2.7) and strong subadditivity. The meaning of this inequality is that conditioning never increases entropy. In other words, knowing the value of Z can never increase our uncertainty about $X|Y$. The former happens when Z confers no information about $X|Y$ and latter when there is correlation, and thus Z can be used to deduce something about the probable value of $X|Y$.

The property (2.8) implies the weaker inequality

$$H(X|Z) \leq H(X) \ , \tag{2.9}$$

if Y is taken to be trivial. This form conveys the same message as (2.8), that additional information never increases uncertainty, in a simpler form.

A related quantity, *mutual information*, quantifies the amount of information that is shared between two systems X and Y. The mutual information is defined

$$I(X, Y) = H(X) + H(Y) - H(X, Y) \ . \tag{2.10}$$

The interpretation of this combination is the following. The sum $H(X) + H(Y)$ counts the total of information contents of X and Y. This sum counts twice any information that is common to both systems, that is, information which is present in both $H(X)$ and $H(Y)$, while counting once any information which appears only in one of the systems. Subtracting $H(X, Y)$, representing information of the composite system, cancels all unique information specific to either X or Y and one copy of the information shared between X and Y, thus leaving behind only one copy of this shared information.

Given this interpretation, one expects $I(X, Y) \geq 0$, with equality when X and Y are not correlated, that is, there is no shared information. This property indeed holds, guaranteed by the subadditivity of Shannon entropy.

2.2 Entanglement in quantum mechanics

2.2.1 Density operator and entangled states

A *density operator*[2] can be used to represent a quantum state, either pure or mixed. Pure states are conveniently described by state vectors, elements of the underlying Hilbert space. A mixed state, which can be understood as a statistical ensemble of pure states, is more conveniently described by a density operator. In practice one is usually working on a mixed state since one is interested in some subsystem of a larger system and there always is interaction between the subsystem and the environment, causing the state of the subsystem to become mixed. The density operator contains complete information about such open quantum systems, analogously to state vectors in the case of pure states/closed systems.

A density operator ρ satisfies the following properties

(i) Self-adjointness: $\rho^\dagger = \rho$

(ii) Non-negativity: $\langle\psi|\,\rho\,|\psi\rangle \geq 0$ for any $|\psi\rangle$

(iii) Unit trace: $\operatorname{tr}\rho = 1$

(iv) $\rho^2 = \rho$ (pure state) or $\rho^2 \neq \rho$ (mixed state) .

The density operator ρ, being Hermitian, can be diagonalized and all its eigenvalues are real. Non-negativity and unit trace additionally imply that all eigenvalues of ρ are non-negative and sum up to unity. A general density operator can be written in the basis of its eigenvectors, $\{|i\rangle\}$, as

$$\rho = \sum_i p_i\,|i\rangle\langle i| \ , \tag{2.11}$$

where $0 \leq p_i \leq 1$ and $\sum_i p_i = 1$. The eigenvalues p_i have the interpretation of assigning probabilities for the system to be in state $|i\rangle$ in the statistical ensemble described by ρ. While it can be useful to think about density matrices as ensembles of pure states, it is important to remember that this ensemble interpretation is not unique. Say we have an ensemble of states $\{p_i, |\psi_i\rangle\}$, meaning that the state $|\psi_i\rangle$ occurs with probability p_i. This corresponds to the density matrix $\rho = \sum_i p_i\,|\psi_i\rangle\langle\psi_i|$. An another ensemble $\{q_i, |\phi_i\rangle\}$ results in the same density matrix, if the states and probabilities are related by

$$\sqrt{p_i}\,|\psi_i\rangle = \sum_j u_{ij}\sqrt{q_j}\,|\phi_j\rangle \ , \tag{2.12}$$

where u_{ij} are components of an unitary matrix. If the sets $\{|\psi_i\rangle\}$ and $\{|\phi_i\rangle\}$ are of different size, the sets may be padded to equal size with zero vectors. The lesson is that for a given density matrix, there is an infinite set of possible ensembles giving rise to it.

[2]We will use the terms density operator and density matrix interchangeably.

Expectation values of operators can be compactly written as

$$\langle O \rangle = \mathrm{tr}(O\rho) = \sum_i p_i \langle i|O|i\rangle \ , \tag{2.13}$$

so an expectation value of $\mathcal{O}$ is the average of individual expectation values of $\mathcal{O}$ in each $|i\rangle$, weighed by the probability associated with that state.

Density matrices in d-dimensional Hilbert space form a convex subset of the space of $d\times d$ Hermitian operators. Consider two density matrices ρ' and ρ''. Then there is an associated infinite family of density matrices

$$\rho(\lambda) = \lambda\rho' + (1-\lambda)\rho'' \ , \tag{2.14}$$

for any $0 \leq \lambda \leq 1$. In contrast to most states, pure states cannot be written in terms of two other density matrices. Other states can be written as linear combinations in multiple ways, and the decomposition (2.11) corresponds to one particular way of forming the linear combination.

A natural way to obtain mixed states is to start with a pure state and trace out some of its parts. Consider a bipartite system, constructed from subsystems A and B, in a pure state. As per the axioms of quantum mechanics, if the individual systems A and B are described by vectors in $\mathcal{H}_A$ and $\mathcal{H}_B$, respectively, then the composite system is described by a vector in $\mathcal{H}_A \otimes \mathcal{H}_B$. A pure composite system can be written $\rho = |\Psi\rangle\langle\Psi|$, with

$$|\Psi\rangle = \sum_{j,k} a_{jk} \, |j\rangle_A \otimes |k\rangle_B \ , \tag{2.15}$$

where the coefficients satisfy $\sum_{j,k} \|a_{jk}\|^2 = 1$ and the vectors $\{|j\rangle_A\}$ and $\{|k\rangle_B\}$ are orthonormal bases of systems A and B, respectively. Any vector in a tensor product space of two Hilbert spaces can be written in a standard form called the *Schmidt decomposition*

$$|\Psi\rangle = \sum_i \sqrt{p_i} \, |i\rangle_A \otimes \left|\tilde{i}\right\rangle_B \ . \tag{2.16}$$

This decomposition can be seen by writing the matrix of coefficients $a_{jk} = u_{ji} d_{ii} v_{ik}$ using a singular value decomposition. The matrices u_{ji}, v_{ik} are unitary and $d_{ii} = p_i$ is a diagonal matrix with non-negative elements. Then, if one defines new states

$$|i\rangle_A = \sum_j u_{ji} \, |j\rangle_A \tag{2.17}$$

$$\left|\tilde{i}\right\rangle_B = \sum_k v_{ik} \, |k\rangle_B \ , \tag{2.18}$$

one ends up with $|\Psi\rangle$ in the Schmidt decomposition (2.16). Since the original basis was orthonormal and the matrices u and v are unitary, $\{|i\rangle_A\}$ and $\left\{\left|\tilde{i}\right\rangle_B\right\}$ are orthonormal as well.

The vector $|\Psi\rangle$ contains maximal information about a closed quantum system. Let us now study what happens in a situation where we are only allowed to observe one part of a larger quantum

system. Say we can observe the subsystem A while B remains inaccessible to us. To see how A appears to us, we need to sum over all possible states of B, or in other words, perform a partial trace of $\rho_{AB} = |\Psi\rangle\langle\Psi|$ over the subsystem B. The resulting density matrix represents our knowledge about the subsystem A by itself and is called a *reduced density matrix*. The reduced density matrix associated with A, denoted by ρ_A, is defined by

$$\rho_A = \mathrm{tr}_B\, \rho_{AB} = \mathrm{tr}_B \left(\sum_{i,j} \sqrt{p_i p_j}\, |i\rangle\langle j|_A \otimes \left|\tilde{i}\right\rangle\left\langle\tilde{j}\right|_B \right) \tag{2.19}$$

$$= \sum_{i,j,k} \sqrt{p_i p_j}\, |i\rangle\langle j|_A \left\langle k\middle|\tilde{i}\right\rangle_B \left\langle\tilde{j}\middle|k\right\rangle_B = \sum_{i,j,k} \sqrt{p_i p_j}\, |i\rangle\langle j|_A \left\langle\tilde{i}\middle|k\right\rangle_B \left\langle k\middle|\tilde{j}\right\rangle_B \tag{2.20}$$

$$= \sum_i p_i\, |i\rangle\langle i|_A \ . \tag{2.21}$$

We started with a general bipartite pure state and ended up with a mixed state of form (2.11). This property is a hallmark of quantum mechanics: the pure state $|\Psi\rangle$ contains maximal information about the composite system but still upon tracing out part of it, one ends up with an ensemble of possible states of the remaining part, each occurring with a probability p_i. When a composite system in a pure state has this property we say that the subsystems A and B are *entangled*. There is nothing special about the subsystem A of course, if we chose to trace out A, we would obtain a reduced density matrix for the subsystem B, $\rho_B = \sum_i p_i \left|\tilde{i}\right\rangle\left\langle\tilde{i}\right|$.

As a simple example of an entangled state consider a pair of two-level quantum systems, or *qubits*, denoted A and B, in the following state

$$|\Psi\rangle = \frac{1}{\sqrt{2}}(|0\rangle_A \otimes |1\rangle_B + |1\rangle_A \otimes |0\rangle_B) \ . \tag{2.22}$$

Let us now find the reduced density matrix associated with the qubit A,

$$\rho_A = \mathrm{tr}_B\, (|\Psi\rangle\langle\Psi|) = \frac{1}{2}(|1\rangle\langle 1|_A + |0\rangle\langle 0|_A) = \frac{1}{2}\mathbb{1}_A \ , \tag{2.23}$$

where $\mathbb{1}_A$ is the identity operator acting on the qubit A. Similarly, for the qubit B one would obtain $\rho_B = \mathbb{1}_B/2$. This means that upon tracing out B, the ensemble describing A contains no information as to in which state the qubit A is. States where the reduced density matrix ρ_A (ρ_B) is proportional to the identity operator once one traces out B (A) are called *maximally entangled*.

The entanglement in state (2.22) has some strange properties as was pointed out by Einstein, Podolsky, and Rosen (EPR) during the formative years of quantum mechanics [12]. Suppose that the two spins are separated by a great distance and a measurement is performed on the qubit A. The outcome of this measurement is $|0\rangle$ half the time and $|1\rangle$ half the time, as in (2.23). Upon measurement of A, the quantum state (2.22) collapses and immediately prepares B in a definite state in such a way, that if B is measured, the results are perfectly correlated with those of A. The objection of EPR to the formulation of quantum mechanics was that this breaks causality. Luckily, this worry is unfounded because causality is still preserved in the sense that entanglement cannot be used for superluminal communications [17, 18].

An another way to characterize entanglement in a composite quantum system is in terms of the *Schmidt number*. The Schmidt number is the number of terms in the Schmidt decomposition (2.16) of a composite system. A pure state is said to be entangled if the Schmidt number is greater than one, otherwise the state is said to be a *product state*. In other words, a product state is one which can be written as

$$|\Psi\rangle_{\text{product}} = |i\rangle_A \otimes \left|\tilde{i}\right\rangle_B \ , \tag{2.24}$$

for some states $|i\rangle_A \in \mathcal{H}_A$ and $\left|\tilde{i}\right\rangle_B \in \mathcal{H}_B$. A pure states can be represented by density matrices

$$\rho_{\text{product}} = \rho_A \otimes \rho_B \ , \tag{2.25}$$

where $\rho_A = |i\rangle\langle i|_A$ and $\rho_B = \left|\tilde{i}\right\rangle\!\left\langle\tilde{i}\right|_B$ are density matrices on $\mathcal{H}_A$ and $\mathcal{H}_B$, respectively.

As a concrete example consider a system of two qubits. One product state would be $|\Psi\rangle = |0\rangle_A \otimes |1\rangle_B$, whereas $|\Psi\rangle = (|0\rangle_A \otimes |1\rangle_B + |1\rangle_A \otimes |0\rangle_B)/\sqrt{2}$ is an entangled state. If a composite system of subsystems A and B are in a product state, the reduced density matrices ρ_A and ρ_B are still definite pure states, as opposed to the case of entangled composite states (2.23). Entangled states are much more common than product states, since in real quantum systems interactions cause different parts of the system to become entangled with one another.

2.2.2 Purification

So far we have only considered bipartite pure states. In this case, detecting entanglement was simple. One only needed to diagonalize one of its reduced density matrices and check whether there is more non-zero Schmidt coefficients than one. It is important to realize that the presence of entanglement is not as clearly diagnosed in the case of mixed states as it is in the case of pure states. A mixed state is said to be *separable* if it can be written as a convex combination of product states

$$\rho_{\text{separable}} = \sum_i p_i \rho_A \otimes \rho_B \ . \tag{2.26}$$

If a mixed state is not a product state nor separable, it is considered to be entangled.

It is in general difficult to tell whether a given state is entangled or separable on the basis of this definition, and a number of criteria for making the distinction have [19].

For any mixed state described by a density operator ρ_A there exists a pure state $|\Psi\rangle$ which reproduces the original mixed density operator when a partial trace is performed. This associated pure state $|\Psi\rangle$ is called a *purification* of ρ_A. If ρ_A is a density operator on $\mathcal{H}_A$, then the purification $|\Psi\rangle$ lives on an extended Hilbert space $\mathcal{H}_A \otimes \mathcal{H}_B$. As per the definition of $|\Psi\rangle$, upon tracing out this extended part of the Hilbert space $\mathcal{H}_B$, the original state is recovered

$$\rho_A = \text{tr}_B \left(|\Psi\rangle\langle\Psi|\right) \ . \tag{2.27}$$

A state $|\Psi\rangle \in \mathcal{H}_A \otimes \mathcal{H}_B$ such that (2.27) holds can always be constructed. Any ρ_A has an orthonormal decomposition $\rho_A = \sum_i p_i |i\rangle\langle i|$. This state can be purified by introducing an auxiliary system $\mathcal{H}_B$

with basis states $\{|i\rangle_B\}$. Now

$$|\Psi\rangle = \sum_i \sqrt{p_i}\,|i\rangle_A \otimes |i\rangle_B \ , \tag{2.28}$$

with $\sum_i p_i = 1$ purifies ρ_A as can be seen by direct computation.

Purification is a mathematical procedure and the introduced auxiliary system need not have any physical meaning but in some cases it can have physical significance. For example, one can purify an open quantum system by considering the environment as the auxiliary system. Since the composite system is closed, it is described by a pure state. One could then perform the Schmidt decomposition of the composite state to obtain a formula analogous to (2.28).

It is important to note that there exists multiple ways to purify a given state. Suppose $|\Psi\rangle \in \mathcal{H}_A \otimes \mathcal{H}_B$ purifies $\rho_A = \sum_i p_i\,|i\rangle\langle i|$. Then one can define an infinite family of purifications by

$$\left|\Psi'\right\rangle = (\mathbb{1} \otimes \mathcal{U})\,|\Psi\rangle \ , \tag{2.29}$$

where $\mathcal{U}$ is an unitary matrix with components u_{ij} in the basis implied by the Schmidt decomposition of $|\Psi'\rangle$. The state $|\Psi'\rangle$ indeed purifies ρ_A

$$\begin{aligned}
\mathrm{tr}_B\left(\left|\Psi'\right\rangle\!\left\langle\Psi'\right|\right) &= \sum_n \sum_{i,j} \sum_{k,l} \sqrt{p_i p_j}\,|i\rangle\langle j|\,\langle n|\,u_{ik}\,|\tilde{k}\rangle\langle\tilde{l}|\,u^\dagger_{nj}\,|n\rangle \\
&= \sum_{i,j} \sqrt{p_i p_j}\,|i\rangle\langle j| \sum_n u_{in} u^\dagger_{nj} \\
&= \sum_i p_i\,|i\rangle\langle i| = \rho_A \ .
\end{aligned} \tag{2.30}$$

The non-uniqueness of purification will be important later when we discuss entanglement of purification.

2.2.3 Von Neumann entropy

Now that we have a criteria for determining whether a quantum state is entangled or not, we should also have ways of quantifying the amount of entanglement in a given state. One would like to find an analogue of the Shannon entropy applicable to quantum states. This notion is provided by the *von Neumann entropy*. Consider a quantum state described by a density operator ρ. The von Neumann entropy is then defined by

$$S(\rho) = \langle -\log_2 \rho \rangle = -\,\mathrm{tr}(\rho \log_2 \rho) \ . \tag{2.31}$$

If one expresses ρ in the basis of its eigenvectors, $\rho = \sum_i p_i\,|i\rangle\langle i|$ the von Neumann entropy can be written $S(\rho) = -\sum_i p_i \log_2 p_i$, which coincides with the Shannon entropy of an ensemble where each eigenstate $|i\rangle$ occurs with probability p_i. In other words, the von Neumann entropy is the Shannon entropy of the spectrum of the quantum state.

A few important properties of the von Neumann entropy are

(i) $S(\rho) \geq 0$ with equality only for a pure state $\rho = |\Psi\rangle\langle\Psi|$.

(ii) Invariant under unitary transformations

$$S(\rho) = S(U\rho U^\dagger) \ , \tag{2.32}$$

since such transformations preserve the eigenvalues of ρ.

(iii) If a state ρ has N non-zero eigenvalues, then

$$S(\rho) \leq \log_2 N \tag{2.33}$$

and the equality saturates for a state where the non-zero eigenvalues all are $1/N$.

(iv) If ρ is a pure state on $\mathcal{H}_A \otimes \mathcal{H}_B$, then the reduced density operators ρ_A and ρ_B satisfy

$$S(\rho_A) = S(\rho_B) \ , \tag{2.34}$$

which is seen from the Schmidt decomposition since both ρ_A and ρ_B have the same eigenvalues.

(v) For any three non-overlapping subsystems A, B, and C, the following inequality is satisfied[3]

$$S(\rho_{ABC}) + S(\rho_C) \leq S(\rho_{AC}) + S(\rho_{BC}) \ . \tag{2.35}$$

This inequality is called *strong subadditivity*.

(vi) If C is empty, the above inequality gives an another inequality

$$S(\rho_{AB}) \leq S(\rho_A) + S(\rho_B) \ , \tag{2.36}$$

which is called *subadditivity*.

(vii) Any bipartite system satisfies the *Araki-Lieb inequality*

$$S(\rho_{AB}) \geq |S(\rho_A) - S(\rho_B)| \ . \tag{2.37}$$

These properties again highlight the difference between quantum mechanics and classical physics. Consider our previous example (2.22), where we found that the reduced density matrices are proportional to unit operators, signalling maximal entanglement (2.23). Even though the composite system is in a definite state, we do not get any information about that state by performing measurements on either of the qubits alone. All information is encoded in nonlocal correlations between qubits.

The Araki-Lieb inequality is curious in comparison to properties of the classical Shannon entropy. While the Shannon entropy of a subsystem never exceeds the entropy of the complete system itself, the Araki-Lieb inequality allows the von Neumann entropies of subsystems to individually have a larger value than their composite system has. Again, this is maximally demonstrated by the two qubit state (2.22), for which $S(\rho_{AB}) = 0$ and $S(\rho_A) = S(\rho_B) = 1$.

[3] Throughout this thesis we will denote set unions by $AB = A \cup B$.

It has been shown that all inequalities satisfied by general bipartite or tripartite systems can be derived from strong subadditivity [20]. Strong subadditivity of the von Neumann entropy was proved in [21]. Strong subadditivity reflects the concavity of the von Neumann entropy and is sufficiently restrictive as a condition to essentially give an unique characterization of the von Neumann entropy [22, 23]. The hierarchy of entropy inequalities changes dramatically when one considers four or more subsystems, in which case there exists an infinite number of independent inequalities for the von Neumann entropy [24].

2.2.4 Measures of entanglement

Having now established the von Neumann entropy as the quantum analogue of the Shannon entropy, let us provide the quantum versions of conditional entropy and mutual information. The definitions are analogous to their classical counterparts

$$S(\rho_A|\rho_B) = S(\rho_{AB}) - S(\rho_B) \tag{2.38}$$

$$I(\rho_A, \rho_B) = S(\rho_A) + S(\rho_B) - S(\rho_{AB}) \ . \tag{2.39}$$

These quantities can be used to measure the correlations between subsystems. A given bipartite system can have both classical and quantum correlations, but the distinction between the two is not straightforward and multiple different notions of the difference have been proposed [25].

The mutual information has the interpretation of measuring the total amount of correlation between subsystems. We say that two systems are correlated if we are less uncertain about the whole than about sum of its parts taken separately. If we take uncertainty about a system to be quantified by entropy, the definition of mutual information is easily understood to measure the amount of this correlation. Furthermore, the non-negativity of the amount of correlation, or mutual information, is guaranteed by the subadditivity of the von Neumann entropy.

As an example consider two qubits in a state $\rho_{AB} = |\Psi^+\rangle\langle\Psi^+|$,

$$\left|\Psi^+\right\rangle = \frac{1}{\sqrt{2}}(|0\rangle_A \otimes |0\rangle_B + |1\rangle_A \otimes |1\rangle_B) \ . \tag{2.40}$$

The two qubits are entangled as $|\Psi^+\rangle$ cannot be written as a product $|\psi\rangle_A \otimes |\psi\rangle_B$. In fact, the qubits are maximally entangled, $\rho_A = \mathrm{tr}_B\, \rho_{AB} = \mathbb{1}_A/2$ and $\rho_B = \mathrm{tr}_A\, \rho_{AB} = \mathbb{1}_B/2$. The entanglement entropy thus takes the maximal value on the subsystems, $S(\rho_A) = S(\rho_B) = \log_2 2 = 1$. Still the composite state is pure, so $S(\rho_{AB}) = 0$ and the mutual information is $I(\rho_A, \rho_B) = 2$. This is an extreme case where all information is encoded in nonlocal entanglement between qubits.

Now consider reducing the correlations between A and B by introducing randomness into the system in the following way. At this point we introduce the conventional characters, Alice and Bob, who possess the systems A and B, respectively. Alice flips a fair coin and if it lands heads, she applies the unitary transformation σ_z on her qubit. The effect of this transformation is to reverse the sign of of her qubit if it is in state $|1\rangle$, otherwise nothing happens. If the coin lands tails, she does nothing. After carrying out this procedure, she forgets whether the coin landed heads or tails and which unitary

operation she applied on her qubit. Now there is a $1/2$ chance the state of the composite system is

$$\left|\Psi^-\right\rangle = \frac{1}{\sqrt{2}}(\left|0\right\rangle_A \otimes \left|0\right\rangle_B - \left|1\right\rangle_A \otimes \left|1\right\rangle_B) \tag{2.41}$$

or still in the initial state (2.40). The pure state ρ has become a mixture

$$\rho'_{AB} = \frac{1}{2}\left|\Psi^+\right\rangle\!\left\langle\Psi^+\right| + \frac{1}{2}\left|\Psi^-\right\rangle\!\left\langle\Psi^-\right| \tag{2.42}$$

$$= \frac{1}{2}\left|0\right\rangle\!\left\langle 0\right|_A \otimes \left|0\right\rangle\!\left\langle 0\right|_B + \frac{1}{2}\left|1\right\rangle\!\left\langle 1\right|_A \otimes \left|1\right\rangle\!\left\langle 1\right|_B \ . \tag{2.43}$$

This state is separable, since it is a mixture of product states. We would say that there is no entanglement, but still there is correlation between the systems. Indeed, were Alice and Bob to perform measurements on their respective qubits, the results would be perfectly correlated. Now the entropy of the joint system is $S(\rho'_{AB}) = 1$ and the mutual information has decreased to $I(\rho'_A, \rho'_B) = 1$. The act of Alice forgetting which operation she performed is essential in this example. After all, Alice performs unitary transformations on her qubit and the von Neumann entropy is invariant under such operations. Forgetting which unitary operator acted on A makes the situation irreversible and increases entropy.

Alice can remove the remaining correlation by flipping the coin once more and applying σ_x if the coin lands heads. This has the effect of flipping her qubit $\left|0\right\rangle_A \leftrightarrow \left|1\right\rangle_A$ with probability $1/2$. Alice again forgets the operation she performed on her qubit after performing it. Now the system is in a product state

$$\rho''_{AB} = \frac{1}{2}\mathbb{1}_A \otimes \frac{1}{2}\mathbb{1}_B \ . \tag{2.44}$$

Now the joint entropy is $S(\rho''_{AB}) = 2$ and all correlations between A and B have been destroyed, as indicated by the mutual information $I(\rho''_A, \rho''_B) = 0$.

A way of making an operational distinction between quantum and classical correlation is the following [26]. The amount of quantum correlation is equal to the amount of randomness one has to introduce to a system in order to make it separable. Classical correlation is the maximal amount of correlation left after removing the quantum correlations. Pure states, as the one in our example above, have equal amounts of quantum and classical correlation by this definition [26].

An another measure of correlation in a quantum state, that is of interest later in this thesis, is the *entanglement of purification*.[4] The von Neumann entropy is essentially unique as an entanglement measure [27], that is, on pure bipartite states all entanglement measures are equal to the von Neumann entropy. For mixed states many measures of classical and quantum correlation are known [19, 28]. To see why using the von Neumann entropy to measure entanglement in mixed states might not be sufficient, consider the mixed state (2.43). This state is a classical mixture of product states and thus not considered to be entangled, but still the entanglement entropy $S(\rho_A)$ is non-zero. The entanglement of purification provides an another way of quantifying correlations in a mixed state. It is a measure of both quantum and classical correlations in a quantum state [29].

[4] Defined below in (2.45).

Consider a density matrix of a bipartite state ρ_{AB} acting on $\mathcal{H}_A \otimes \mathcal{H}_B$. Let the purification of this state be $|\Psi\rangle \in \mathcal{H}_{AA'} \otimes \mathcal{H}_{BB'}$. The entanglement of purification $E_P(\rho_{AB})$ is defined as

$$E_P(\rho_{AB}) = \min_{|\Psi\rangle} S(\rho_{AA'}) \ , \tag{2.45}$$

where the minimization is taken over all purifications of ρ_{AB}. In the definition of E_P we could equivalently use $S(\rho_{BB'})$ instead of $S(\rho_{AA'})$ since the state $|\Psi\rangle$ is pure. $E_P(\rho_{AB})$ is bounded from below by mutual information divided by two,

$$E_P(\rho_{AB}) \geq \frac{I(\rho_A, \rho_B)}{2} \ . \tag{2.46}$$

Further properties of $E_P(\rho_{AB})$ can be found in [30]. Entanglement of purification has applications in quantum communication and quantum error correction but these applications are outside of the scope of this thesis [31].

2.3 Entanglement in quantum field theory

Most of the concepts introduced in the previous section carry over to the context of QFTs by thinking of taking a continuum limit of the theory defined on a discrete lattice. States of QFTs can be expressed in terms of path integrals where field configurations are integrated over with a weight given by the action of the theory. One may then imagine taking the resulting density matrix and tracing out a part of the total Hilbert space and then calculating the von Neumann entropy of the resulting reduced density matrix ρ_A to characterize entanglement in the QFT state. Omitting the technicalities of calculating a logarithm of a continuum operator, one can imagine diagonalizing ρ_A to find its spectrum which gives the entanglement entropy. A bigger difficulty in QFTs is that the spatial bipartitioning, required by our wish to find the entanglement associated to a spatial region, does not necessarily have a neat correspondence to a bipartitioning of the total Hilbert space. If there are no gauge symmetries, one can think of the Hilbert space as a product of Hilbert spaces associated to individual spatial points and bipartition the Hilbert space to $\mathcal{H}_A \otimes \mathcal{H}_{A^c}$.[5] In the case of gauge theories such bipartitioning turns out to be impossible [32–35]. The reason for this is that in gauge theories, excitations are associated with closed loops instead of points in space [36–38]. All of these loops cannot be associated with either A or A^c alone since there exist loops that cross the entangling surface. We will omit this technicality by implicitly assuming that a convention has been adopted for dealing with the problematic degrees of freedom.

2.3.1 Area law of entanglement entropy

An important difference compared to discrete systems is that the entanglement entropy is divergent due to degrees of freedom lying very close to ∂A but still on opposite sides of it. This happens because QFTs tend to be local, that is, their constituents interact primarily with their nearest neighbours. The

[5] We will denote a complement with a superscript, e.g., A^c.

locality of interactions leads to correlations that are strong between nearby degrees of freedom and decay for larger distances. This divergence can be removed by introducing a UV cutoff to regulate correlations between degrees of freedom just on the opposite sides of the entangling surface. This leads us to expect a leading divergence of entanglement entropy in a QFT living on a d-dimensional spacetime to have the form [39]

$$S(\rho_A) = \gamma \frac{Vol(\partial A)}{\epsilon^{d-2}} + \dots \ , \tag{2.47}$$

where ϵ is the cutoff for regulating correlations across the codimension-2 entangling surface. This type of a divergence is called an *area law*, since it is proportional to the area of the entangling surface. The area law is a common feature in QFTs but it can be violated. Violations can be observed in some fermionic systems [40–42] and in QFTs which have nonlocal interactions and the region considered has size smaller than the length scale of the nonlocality [43, 44]. An another way to have area law violating nonlocality is to study noncommutative QFTs [45, 46]. We have studied entanglement entropy and various other quantities in a noncommutative QFT in the included paper [III].

Let us now focus on local quantum field theories. If the entangling surface ∂A is smooth, we expect that the divergences in $S(\rho_A)$ should only depend on local physics at the entangling surface. Then the divergence should be expressible as an integral over ∂A such that the value of the integrand at any point depends only on the local geometric invariants of ∂A

$$S(\rho_A)^{\text{div}} = \int_{\partial A} d^{d-2}\sigma \sqrt{h} F(K_{ab}, h_{ab}) \ , \tag{2.48}$$

where $F(K_{ab}, h_{ab})$ gives the sum of all local geometric invariants built from the extrinsic curvature K_{ab} and induced metric h_{ab} at a given point in ∂A [47]. It can be then argued that the entanglement entropy across a smooth, scalable surface in general has a UV-behaviour [47]

$$S(\rho_A) = \begin{cases} a_{d-2}\left(\frac{R}{\epsilon}\right)^{d-2} + a_{d-4}\left(\frac{R}{\epsilon}\right)^{d-4} + \dots + (-1)^{\frac{d-1}{2}} s_d + \mathcal{O}(\epsilon) & d \text{ odd} \\ a_{d-2}\left(\frac{R}{\epsilon}\right)^{d-2} + a_{d-4}\left(\frac{R}{\epsilon}\right)^{d-4} + \dots + (-1)^{\frac{d-2}{2}} s_d \log\frac{R}{\epsilon} + \text{const} + \mathcal{O}(\epsilon) & d \text{ even} \ , \end{cases} \tag{2.49}$$

where R is a length scale characterizing the size of the entangling surface ∂A. Later when we are considering holographic theories where practical entanglement computations are feasible, we must prepare ourselves for encountering and regularizing the above divergences. We will see that the area law divergence of entanglement entropy will arise elegantly in the holographic context.

2.3.2 Singular entanglement surfaces

We have already stated that the UV-behaviour (2.49) can be avoided by giving up locality in the QFT, e.g. by introducing noncommutativity in the spacetime. Another way in which (2.49) might fail is for entangling regions which are not smooth [48, 49]. A two-dimensional entangling region can have sharp corners. In higher dimensions, the entangling region can have geometrical singularities that look locally like creases or cones, see Fig. 2.1. In these cases, the entanglement entropy receives

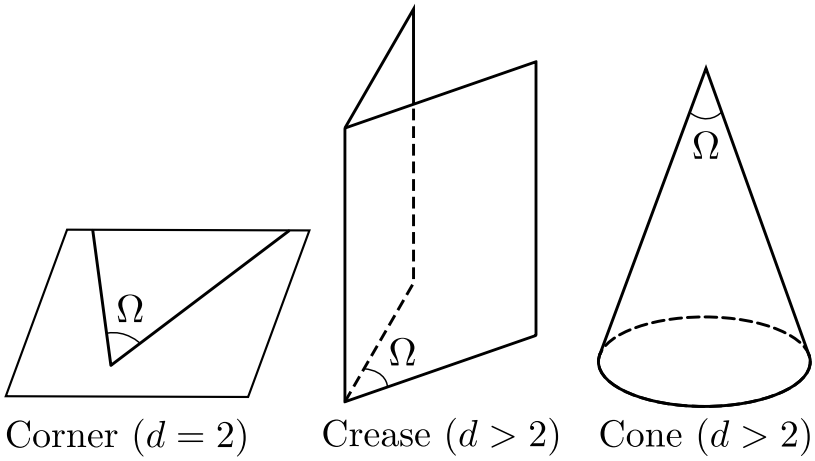

Figure 2.1: Three different entangling surfaces with geometrical singularities. The basic type of singularity in two spatial dimensions, that is, for one-dimensional entangling surfaces is the corner (left). An arbitrary one-dimensional entangling surface is formed by a number of corners and smooth sections connecting them. In higher dimensions, entangling surfaces can have different singular loci. For example, the crease (middle) and the cone (right) represent different extensions to higher dimensions. Note that in the case of the cone, we define Ω to be the angle of the plane section of the cone instead of a solid angle. In this way all of these singular surfaces reduce to smooth ones for $\Omega \to \pi$.

contributions of the form

$$a^{(d)}(\Omega) \log \frac{R}{\epsilon} \,, \tag{2.50}$$

where $a^{(d)}(\Omega)$ is a function that encodes the effect of the geometric singularity characterized by an opening angle Ω. The function $a^{(d)}(\Omega)$ depends on the spacetime dimension d and the type of the singular surface. Different singular surfaces and dimensions may produce terms which differ in sign, or can have a different power for the logarithm (2.50). The function is such that in the limit $\Omega \to \pi$ it vanishes since in this limit the entangling surface becomes smooth. If one considers a pure state, then $a^{(d)}(\Omega) = a^{(d)}(2\pi - \Omega)$ because $S(\rho_A) = S(\rho_{A^c})$ must hold. For an explicit example of the computation of entanglement entropy for a singular entangling surface, see the included paper [I].

2.3.3 Renormalization group flow and c-theorems

The *renormalization group* is a tool in quantum field theory for studying how a given physical system behaves at different scales. Consider a QFT with an action functional

$$S(g, \epsilon) = \int \mathcal{L}(g, \epsilon, x) d^d x \,, \tag{2.51}$$

where ϵ is a UV-cutoff, $x = \{x_0, x_1, \dots\}$ are the spatial coordinates and $g = \{g_0, g_1, \dots\}$ is a set of parameters or coupling constants. The renormalization group flow is a single-parameter group of scale

transformations R_t in the space of coupling constants Q. This flow is such that a QFT described by the action $S(R_t g, e^t \epsilon)$ is equivalent to the original QFT described by $S(g, \epsilon)$ in the sense that their correlation functions agree at scales much larger than the new cutoff $x \gg e^t \epsilon$, with $t > 0$. The vector field generating this flow in Q is given by a set of β-functions which describe how a coupling changes as a function of t,

$$\frac{dg_i}{dt} = \beta_i(g) \ . \tag{2.52}$$

Renormalization group (RG) flow following this rough prescription can be used in most QFTs of interest, with the notable exception of gravity. Observables in the QFT change in magnitude when studied at larger scales, some always increase (relevant observables), some always decrease (irrelevant observables), and some neither increase or decrease (marginal observables). In general, there are points along the RG flow where the β functions vanish. These correspond to points of scale invariance in G where the physical system is described by a conformal field theory (CFT).

For QFTs in two spacetime dimensions, there is a *c-theorem* which tracks the number of degrees of freedom along their RG-flows [50]. The c-theorem states that there exists a function $c(g)$ on the space of coupling constants G such that $c(g)$ monotonically decreases along the RG flow and is stationary at the fixed points, where the value of $c(g)$ equals the central charge of the corresponding CFT. The central charge of a CFT is understood as a measure of the number of degrees of freedom in the theory. As a consequence of the c-theorem we know that if two fixed points are connected by an RG flow, then the c-function has a higher value at the UV fixed point than at the IR-fixed point. This reflects the intuition that the number of degrees of freedom in a QFT should decrease when short distances are integrated out by the RG transformation.

Similar c-theorems have been searched for in higher dimensions. There is a c-theorem in even dimensions [51] that passed many non-trivial tests in four spacetime dimensions [52–55] and was later proved [56]. This theorem is known as the *a-theorem* since the role of the $c(g)$ function is played by a function $a(g)$.[6] These even dimensional c-theorems rely on the existence of trace anomalies which are not present in odd dimensions. In three spacetime dimensions, a *F-theorem* has been conjectured based on the observed monotonicity along RG flow of the free energy on a three sphere in certain QFTs [57]. The F-theorem is conjectured to hold in all three-dimensional QFTs, and it has been shown to hold in various cases [58–60]. Further, there are connections between the F-theorem and the entanglement entropy on the three sphere [61, 62].

The ideas of RG flow, c-theorems, and entanglement entropy are recurring themes in the papers included in this thesis. We have studied entanglement entropy and c-functions derived from it in a QFT which enables practical computations of observables along a RG flow between two conformal fixed points [II]. We have also studied other information theoretic quantities, such as the mutual information and entanglement of purification, along RG flows [I].[7]

[6] Note that there is no relation to the function in (2.50).

[7] Entanglement of purification is computed via its proposed holographic dual, the entanglement wedge cross section.

Chapter 3

Holographic entanglement entropy

It has been suspected for some time now that the degrees of freedom in quantum gravity must be organized in such a way that they can be equivalently described by a non-gravitational quantum many-body system in one lower spatial dimension [5, 6]. This radical reduction in the number of degrees of freedom compared to the naive expectation was discovered by noting that the entropy associated with a spatial region filled with particles must be proportional to the area of its boundary, since a black hole can always be formed by throwing in additional matter. The entropy of a black hole is famously given by the Bekenstein-Hawking formula [4, 63], which states that the entropy of a black hole is proportional to the area of its event horizon. This observation is the basis of the *holographic principle* which conjectures that it is a general property of quantum gravity that all information about a spatial volume is encoded on its boundary.

The AdS/CFT correspondence [3] is the first explicit realization of the holographic principle. AdS/CFT gives an example of a duality, or physical equivalence, between two seemingly unrelated quantum systems. It is a correspondence between a standard theory of quantum fields and a theory of quantum gravity, where the collective dynamics of the former give rise to the gravitational degrees of freedom of the latter [64–66]. The way in which this dual spacetime emerges from standard QFT dynamics has ties to entanglement properties of the QFT state considered.

Methods for computing the entanglement entropy in quantum field theories involve calculating highly complicated functional integrals over singular branched manifolds. Computing such integrals is an intimidating task and explicit calculations can be carried out only in a few particularly simple situations where either symmetry or lack of interaction comes to the rescue. In free field theories there are examples where explicit computations are possible [39, 67]. An another class of tractable systems is provided by exploiting conformal symmetry in two spacetime dimensions [68]. Still, in general interacting quantum field theories the task of computing the entanglement entropy remains intractable.

Holographic dualities make it possible to translate the problem of finding the entanglement entropy in a QFT to an equivalent but simpler problem on the gravity side of the correspondence. In the limit of strong coupling and large number of degrees of freedom, a holographic QFT can be described by classical gravity. Entanglement entropy can be calculated in gravity with a spectacularly simple

formula proposed by Ryu and Takayanagi [69]. The proposal states that the entanglement entropy is given by the area of a certain surface in the gravity background. This is a massive simplification over the equivalent calculation in the field theory side and makes it practical to study entanglement in ways that was previously impossible.

This thesis is primarily concerned with using the proposal of Ryu and Takayanagi for practical calculations for entanglement entropy and related quantities. The QFTs we will study in this chapter and the included papers are dual to spacetimes that are at least asymptotically anti-de Sitter spaces. The notable exception to this is our study of entanglement entropy in a noncommutative QFT in which case the nonlocality at the scales set by the noncommutative parameter deforms the UV away from the CFT fixed point represented by the asymptotically AdS metric [III]. All the backgrounds we work with are presented in detail in the included papers and in earlier original works [70–74].

We will first start by discussing what the anti-de Sitter space is and what kind of properties it has. Then we will discuss the holographic entanglement entropy proposal of Ryu and Takayanagi in detail, giving also explicit examples to its use. Finally we will discuss holographic realizations of some other information theoretic quantities, such as mutual information and entanglement of purification.

3.1 Properties of anti-de Sitter spacetime

The anti-de Sitter spacetime is at the center stage in the papers included in this thesis, so in this section we briefly recall some of its most important properties. Consistently with the rest of this thesis, we will now work in $d+1$ spacetime dimensions. One should note that the backgrounds in the included papers are in many cases derived from string theory, meaning that the spacetimes are ten-dimensional. The spacetimes are such that some dimensions are compact, forming an internal space. Noncompact dimensions on the other hand are typically asymptotically AdS where the non-AdS nature of the interior reflects the nonconformal nature of the dual QFT at these scales. However, in this introduction we will suppress the internal dimensions since this reduces complexity and still enables us to showcase the properties we wish to introduce.

Anti-de Sitter spacetime is one of three maximally symmetric Lorentzian signature solutions to Einstein's equations. Maximally symmetric solutions are those spacetimes which have the maximal amount of Killing vectors, $(d+1)(d+2)/2$ in $d+1$ spacetime dimensions. The maximally symmetric solutions are distinguished by the sign of their curvatures. Minkowski, de Sitter, and anti-de Sitter spacetimes correspond to zero, positive, and negative curvatures, respectively. They are the Lorentzian counterparts of the Euclidean space, sphere, and hyperboloid, respectively.

Anti-de Sitter space can be defined as a pseudosphere in $\mathbb{R}^{d,2}$

$$-(X_0)^2 - (X_{d+1})^2 + \sum_{i=1}^{d}(X_i)^2 = -L^2 \ , \tag{3.1}$$

where L is the radius of curvature of AdS_{d+1}. This equation defines a set of points equidistant from

the origin as measured by the ambient metric

$$g = -dx_0^2 - dx_{d+1}^2 + \sum_{i=1}^{d} dx_i^2 \ . \tag{3.2}$$

The ambient metric and the defining equation of the pseudosphere are invariant under $SO(d,2)$ rotations around the origin, so the AdS_{d+1} has the isometry group $SO(d,2)$ inherited from the embedding space. Anti-de Sitter space has the topology $S^1 \times \mathbb{R}^d$ which can be seen by writing (3.1) as

$$(X_0)^2 + (X_{d+1})^2 = L^2 + \sum_{i=1}^{d} (X_i)^2 \ . \tag{3.3}$$

Now consider fixing a point on the plane $X_1, \ldots, X_d$. Then the above equation states that through each of these points, AdS has a closed circle in the (X_0, X_{d+1}) timelike plane, that is, a closed timelike curve. Later we will try to alleviate concerns about closed timelike curves by passing to the universal covering space of (3.1) effectively by replacing the S^1 with $\mathbb{R}$. It is precisely this covering space that is usually referred to by anti-de Sitter spacetime. In AdS/CFT, bulk classical gravity is isomorphic to the dual QFT, so in particular, the same symmetries must be realized on both sides of the correspondence. This is indeed the case: the $SO(d,2)$ group of isometries of AdS_{d+1} matches the conformal group of the QFT in d dimensions.

In our applications, the two most important coordinate charts are the *global coordinates* and the *Poincaré coordinates*. Global coordinates are defined by parametrizing the pseudosphere (3.1) by

$$X_0 = L \sin\frac{\tau}{L} \cosh\frac{\rho}{L} \ , \quad X_{d+1} = L \cos\frac{\tau}{L} \cosh\frac{\rho}{L} \tag{3.4}$$

$$X_i = L \sinh\frac{\rho}{L} \Omega_i \ , \quad i = 1, \ldots, d \ , \tag{3.5}$$

where Ω_i are components of an unit vector on a S^{d-1}, parameterized by the usual $d-1$ angular variables. This parametrization makes sense because it is chosen in such a way that

$$(X_0)^2 + (X_{d+1})^2 = L^2 \cosh^2\frac{\rho}{L} \tag{3.6}$$

$$\sum_{i=1}^{d} (X_i)^2 = L^2 \sinh^2\frac{\rho}{L} \ . \tag{3.7}$$

The temporal coordinate τ is chosen to be the angle parametrizing the S^1 and Ω_i contain the angular coordinates on S^{d-1}. In these coordinates, the induced metric on AdS_{d+1} is

$$g = -\cosh^2\frac{\rho}{L} d\tau^2 + d\rho^2 + L^2 \sinh^2\frac{\rho}{L} d\Omega_{d-1}^2 \ , \tag{3.8}$$

with $\rho \in [0, \infty)$.[1] These coordinates show explicitly the closed timelike curves in AdS. The temporal coordinate winds around the embedding hyperboloid (3.1) with period 2π. In the universal covering

[1] We follow the convention where all metrics have mostly plus signature.

space, where we will work most of the time, one does not identify $\tau \sim \tau + 2\pi$ and takes $\tau \in \mathbb{R}$ instead.

A different radial coordinate is also commonly used in the global patch of AdS. If one defines a radial coordinate r by

$$\frac{r}{L} = \sinh \frac{\rho}{L} \ , \tag{3.9}$$

then the AdS_{d+1} metric becomes

$$g = -\left(1 + \frac{r^2}{L^2}\right) d\tau^2 + \frac{dr^2}{1 + \frac{r^2}{L^2}} + r^2 d\Omega_{d-1}^2 \ , \tag{3.10}$$

which has the advantage of having a familiar form in that it looks like a Schwarzschild black hole with a blackening factor $f(r) = 1 + r^2/L^2$. In this form it is also explicit that in the limit of large radius of curvature $L \to \infty$, the anti-de Sitter space approaches the flat Minkowski space.

We will introduce an another radial coordinate for the global patch in order to draw the Penrose diagram of AdS. The goal is to find a radial coordinate in which (3.8) has equal prefactors for temporal and radial directions. This is accomplished by defining $\sigma = \operatorname{arcsin} \tanh(\rho/L)$ which brings the metric (3.8) to the form

$$g = \frac{1}{\cos^2 \alpha} \left(-d\tau^2 + d\sigma^2 + \sin^2 \alpha d\Omega_{d-1}^2\right) \tag{3.11}$$

$$= \frac{1}{\cos^2 \alpha} \left(-d\tau^2 + d\Omega_d^2\right) \ , \tag{3.12}$$

where $d\Omega_d^2$ denotes the standard metric on S^d. Note that the range of α is $[0, \pi/2)$, meaning that slices of constant time are half-spheres. The conformal boundary at $\alpha = \pi/2$, where in the context of the AdS/CFT correspondence the field theory lives, has a Lorentzian signature and topology $\mathbb{R} \times S^{d-1}$. The conformal boundary can be regarded as the conformal compactification of Minkowski space where the point at the spatial infinity has been added. Omitting the transverse S^{d-1}, the Penrose diagram for AdS_{d+1} is an infinite strip extending in the time direction, shown in Fig. 3.1. From the Penrose diagram one can see that some properties of AdS are quite different compared to the more usual, asymptotically flat spacetimes. AdS has a Lorentzian boundary, which can be reached by light rays in finite coordinate time. This is in stark contrast with asymptotically flat spacetimes where there are distinct lightlike and spacelike infinities. Also, it shows in a nice way that AdS is not globally hyperbolic. Indeed, it can be seen that no spatial slice has all of AdS in its domain of dependence. For any spacelike surface Σ there exists points to the future of Σ such that past directed causal curves do not necessarily intersect Σ, because they will hit the conformal boundary instead. We can still have well defined time evolution if we supplement the initial conditions on Σ with boundary conditions that define what happens when a light ray hits the boundary of AdS. A common prescription is to consider reflective boundary conditions, where a light ray is reflected back into the bulk when it hits the boundary.

Timelike geodesics in AdS are such that if two of them start from the same point at $\tau = 0$, they will first diverge until $\tau = L\pi/2$ where they will turn back and finally converge at $\tau = L\pi$. If one thinks

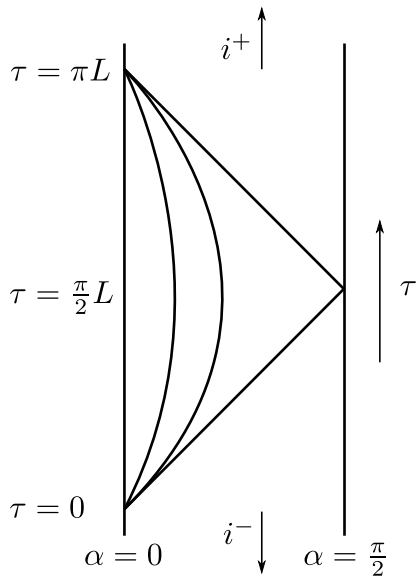

Figure 3.1: Penrose diagram of anti de-Sitter space. The center of AdS is represented by $\alpha = 0$ and the boundary lies at $\alpha = \pi/2$. The diagram extends infinitely in the temporal direction and $i^{\pm}$ represent the timelike infinities. The lines originating from $\tau = \alpha = 0$ are geodesics. The null geodesic reaches the boundary and is reflected back while the timelike geodesics turn back at a finite distance from the center. The geodesics converge after time $\tau = \pi L$.

of AdS as a pseudosphere embedded in $\mathbb{R}^{d,2}$, the geodesics are circles around the sphere. Geodesics converging at time $\tau = L\pi$ corresponds to the circles intersecting at the point on the sphere antipodal to the initial point. After time $\tau = 2\pi L$ the geodesics converge again, this time at the initial point and then continue to alternate between diverging and converging infinitely. No timelike geodesic can reach the boundary of AdS as they are all bound to return to their initial points after moving a finite distance towards the boundary [75].

One further coordinate system on AdS must still be introduced. These are the *Poincaré coordinates*, which are commonly used in the literature. This time we parametrize the embedded pseudosphere (3.1) with a new radial coordinate z and a set $x^\alpha = \{t, x, y, \dots\}$ corresponding to coordinates on the conformal boundary. These coordinates are defined by

$$X_0 = \frac{1}{2z}\Big(L^2 + \eta_{\alpha\beta}x^\alpha x^\beta\Big), \quad X_{d+1} = \frac{1}{2z}\Big(L^2 - \eta_{\alpha\beta}x^\alpha x^\beta\Big) \,, \tag{3.13}$$

$$X_i = L\frac{x^i}{z} \,, \quad i = 1, \dots, d \,, \tag{3.14}$$

where $x^\alpha \in \mathbb{R}$, $z > 0$ and η is the Minkowski metric. This time the metric reads

$$g = \frac{L^2}{z^2}\Big(dz^2 + \eta_{\alpha\beta}dx^\alpha dx^\beta\Big) \,. \tag{3.15}$$

The conformal boundary lies at $z = 0$. Another common parametrization of the radial direction is to use $r = 1/z$, in which case the boundary is at $r \to \infty$.[2] Sometimes in the literature, z is called r, usually in contexts where z already has some other meaning. The advantage of Poincaré coordinates is that the metric is proportional to the metric of a flat Minkowski spacetime with a proportionality factor that is a simple function of the radial coordinate only. In Poincaré coordinates, many symmetries of the system are explicit. The metric (3.15) has explicit Poincaré invariance and invariance under dilatations where all coordinates are multiplied by a common positive factor. In the context of the AdS/CFT correspondence, the Poincaré and dilatation symmetries of the bulk are related to the conformal symmetry of the boundary theory, which is why it is convenient to have the symmetries manifest themselves in a simple way on the bulk side.

It is important to note that Poincaré coordinates only cover one half of the AdS manifold. One way to see this is to notice that $X_0 + X_{d+1} = \frac{L^2}{z} > 0$. Another way is to consider radial null geodesics directed towards the center of AdS, that is, towards $z \to \infty$ or $r \to 0$. They will reach $z = \infty$ or $r = 0$ at a finite value of the affine parameter of the geodesic and escape the region of space covered by our coordinates. This region is called the *Poincaré patch* and the surface $z = \infty$ or $r = 0$ is called the *Poincaré horizon*. To cover all of the AdS manifold, one needs two Poincaré charts, one for $z > 0$ and another for $z < 0$. For a careful analysis on the relationship between global and Poincaré boundaries of AdS, see [76].

One further property of AdS needs to be commented on: its stability or lack thereof. The two other maximally symmetric spaces, Minkowski and de Sitter space, are stable linearly and nonlinearly [77, 78]. These proofs cover also asymptotically Minkowski and de Sitter spaces. Conceptually, stability of these spaces follows from the fact that perturbations can escape to infinity and disperse in a way that the metric is not modified substantially. The situation is dramatically different in AdS. As discussed previously, no timelike geodesic can ever reach the boundary. That is, any massive particle will always return to its starting point in finite time irrespective of their initial velocity towards the boundary. Same is true of photons. Even though null geodesics will reach spatial infinity in finite coordinate time, they will reflect back into the bulk due to reflective boundary conditions at the boundary, imposed in order to prevent photons from escaping AdS and removing energy from the spacetime. Thus, the curvature of AdS is such that it acts like a gravitational potential well with mirrors as its boundaries. This particle trapping behaviour breaks the property that makes Minkowski and de Sitter spaces stable, forcing particles to oscillate infinitely instead of dispersing to infinity. It is now known that AdS is nonlinearly unstable for large classes initial data. There are islands of stability in the space of initial conditions, but for many initial conditions, AdS seems to be unstable against gravitational collapse even for perturbations with arbitrarily small amplitudes. What tends to happen is that energy of the initial configuration flows to higher frequency spatial modes and eventually, when the energy is concentrated enough, collapses to an AdS-Schwarzschild black hole [79–87].

Since much of the interest in the properties of AdS spacetime is driven by the AdS/CFT correspondence, it is natural to ask what the instability of AdS means on the dual field theory side. From the

[2] Note that this r-coordinate is different from the one introduced in (3.9) for the global patch.

point of view of the field theory, the instability is not all that surprising. After all, one would expect any perturbation of a field theory to eventually thermalize and the endpoint of the instability is a black hole in AdS, which is dual to a thermal state in the QFT. However, the islands of stability mentioned before show that this expectation is not completely true either. There are initial conditions which instead of collapsing to form a black hole, form periodic, oscillating solutions [88–91]. These bulk solutions correspond to boundary states that fail to thermalize. Even in the case where some initial data does collapse to a black hole, it necessarily does not mean that the field theory has thermalized. If the spacetime does not have enough energy to form a sufficiently large black hole, the black hole may be unstable and radiate away leaving behind a pure AdS space [92]. These small black holes in AdS space are interesting objects that can appear as unstable phases between two stable phases, for example, in between confined and deconfined phases [93]. For more about the properties of small black holes in the context of the AdS/CFT correspondence, see the included paper [IV] where we study the behaviour of correlation functions interpolating between stable black hole and thermal AdS phases.

3.2 Holographic entanglement entropy proposal

The gauge/gravity duality gives a spectacularly simple way to calculate the entanglement entropy of a QFT by performing the calculation on the gravity side of the duality. The prescription for how to do this in static gravitational backgrounds was proposed by Ryu and Takayanagi [69, 94]. Their proposal became to be known as the RT-prescription. Subsequently the RT-prescription was extended to time-dependent backgrounds by Hubeny, Rangamani, and Takayanagi [95]. This extension is known as the HRT-prescription.

Consider a holographic QFT on a d-dimensional manifold $\mathcal{B}_d$. The quantum gravity dual in the classical limit is a $(d+1)$-dimensional, asymptotically AdS_{d+1}, manifold $\mathcal{M}_{d+1}$ such that $\partial\mathcal{M}_{d+1} = \mathcal{B}_d$. For now we are assuming that the bulk manifold $\mathcal{M}_{d+1}$ is static, admitting a timelike Killing field, which defines a canonical foliation for $\mathcal{M}_{d+1}$ and $\mathcal{B}_d$ with spacelike surfaces. We are now interested in the entanglement entropy associated with a region A lying on a time slice of $\mathcal{B}_d$. Here we are assuming that at this instant of time, the Hilbert space of the QFT can be divided to $\mathcal{H}_A \otimes \mathcal{H}_{A^c}$, where $\mathcal{H}_A$ is the Hilbert space associated with the spatial region A. This setup is shown in Fig. 3.2.

Now the prescription tells us to consider a codimension-2 bulk surface Σ_A, which satisfies

- Σ_A is anchored on A: $\partial\Sigma_A = \partial A$
- Σ_A is homologous to A .

The homology condition means that there exist a codimension-1 bulk interpolating surface bounded by Σ_A and A. In other words, the bulk surface Σ_A should be smoothly retractable to A on the boundary. The prescription for computing $S(A)$ is to select the surface Σ_A which simultaneously

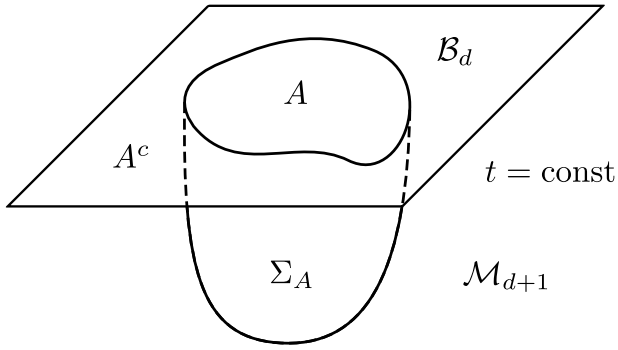

Figure 3.2: The bulk setup for computing $S(A)$ with the RT-prescription. A constant time slice of the boundary is partitioned into A and its complement A^c. The bulk surface Σ_A is such that it anchors on the boundary of A and minimizes its volume by extending into the bulk. The entanglement entropy is then given by the volume of Σ_A as in (3.16).

satisfies the above constraints and has minimal volume[3]. Then the holographic entanglement entropy is the volume of this surface in Planck units[4]

$$S(A) = \frac{1}{4G_N^{(d+1)}} \min_{\Sigma_A} Vol(\Sigma_A) \ . \tag{3.16}$$

In section 2.3 we saw that short range correlations in a QFT lead naturally to an area law divergence, that is, a divergence in entanglement entropy proportional to the volume of the entangling surface. This area law appears elegantly from the RT-proposal as can be seen directly from (3.16). The formula diverges because of the infinite volume of AdS_{d+1}, and the divergence originates from the part of Σ_A that anchors on the boundary. The bulk minimal surface touches the AdS_{d+1} boundary only at $\partial\Sigma_A = \partial A$, and thus the divergence must be proportional to $Vol(\partial A)$, giving a simple, geometric intuition for the leading divergence structure of entanglement entropy.

The RT-proposal massively simplifies the calculation of entanglement entropy in interacting QFTs, reducing the task to finding a minimal surface in a curved spacetime. Geometric intuition makes it easy to prove that the RT-proposal satisfies the properties it should, some of which we will now show.

The von Neumann entropy is always nonnegative for any state. Nonnegativity is manifest in (3.16) as it is formulated as the volume of a surface on a spacelike spatial slice of a manifold.

For a pure state $\rho = |\Psi\rangle\langle\Psi|$, the entanglement entropy must satisfy $S(A) = S(A^c)$ for any bipartition $\rho_A = \mathrm{tr}_{\mathcal{H}_{A^c}} \rho$. This property is clearly satisfied by (3.16) since the surfaces Σ_A and Σ_{A^c} are solely determined by their shared entangling surface, $\partial A = \partial A^c$. This results in the exact same minimal surface for both A and A^c, implying $S(A) = S(A^c)$.

An another important property of entanglement entropy is strong subadditivity, the proof of which

[3]In this chapter, we denote the entanglement entropy associated to region A by $S(A)$, instead of $S(\rho_A)$ which was used in Chapter 2.

[4]In our units $\hbar = c = 1$, the gravitational constant is proportional to the Planck area: $G_N^{(d+1)} \sim l_P^2$.

we now outline [96]. This also is a nice example of a simple, holographic proof of an inequality that would be quite involved to prove directly on the field theory side. Strong subadditivity

$$S(a \cup c) + S(b \cup c) \geq S(a \cup b \cup c) + S(c) \tag{3.17}$$

is an inequality concerning three reduced density matrices which in our QFT context correspond to spatial regions a, b, and c. This inequality can be equivalently expressed with two overlapping regions defined by

$$A = a \cup c \ , \quad B = b \cup c \ . \tag{3.18}$$

With this redefinition, the strong subadditivity becomes

$$S(A) + S(B) \geq S(A \cup B) + S(A \cap B) \ . \tag{3.19}$$

Let Σ_A^{min} and Σ_B^{min} be the minimal bulk surfaces associated with the boundary regions A and B. The corresponding bulk regions, denoted by $\mathcal{R}_A$ and $\mathcal{R}_B$, satisfy $\partial\mathcal{R}_A = A \cup \Sigma_A^{\text{min}}$ and $\partial\mathcal{R}_B = B \cup \Sigma_B^{\text{min}}$. Now let $\mathcal{R}_{A\cup B} = \mathcal{R}_A \cup \mathcal{R}_B$ and $\mathcal{R}_{A\cap B} = \mathcal{R}_A \cap \mathcal{R}_B$. We define the associated bulk surfaces $\Sigma_{A\cup B}$ and $\Sigma_{A\cap B}$ by the equalities

$$\Sigma_{A\cup B} : \partial\mathcal{R}_{A\cup B} = A \cup B \cup \Sigma_{A\cup B} \tag{3.20}$$

$$\Sigma_{A\cap B} : \partial\mathcal{R}_{A\cap B} = (A \cap B) \cup \Sigma_{A\cap B} \ . \tag{3.21}$$

These surfaces are anchored to $A \cup B$ and $A \cap B$, respectively, $\partial\Sigma_{A\cup B} = \partial(A \cup B)$ and $\partial\Sigma_{A\cap B} = \partial(A \cap B)$. The surfaces $\Sigma_{A\cup B}$ and $\Sigma_{A\cap B}$ are clearly formed by cutting and pasting parts of the original minimal surfaces Σ_A^{min} and Σ_B^{min} and thus their total area must be preserved in the rearrangement,

$$Vol(\Sigma_A^{\text{min}}) + Vol(\Sigma_B^{\text{min}}) = Vol(\Sigma_{A\cup B}) + Vol(\Sigma_{A\cap B}) \ . \tag{3.22}$$

However, since neither $\Sigma_{A\cup B}$ and $\Sigma_{A\cap B}$ are guaranteed to be the minimal area surfaces of the corresponding boundary regions $A \cup B$ and $A \cap B$, we have

$$Vol(\Sigma_{A\cup B}) + Vol(\Sigma_{A\cap B}) \geq Vol(\Sigma_{A\cup B}^{\text{min}}) + Vol(\Sigma_{A\cap B}^{\text{min}}) \ , \tag{3.23}$$

where on the right hand side we have the bulk surfaces which actually have minimal area. By combining the above relations and expressing surface areas in terms of the corresponding entanglement entropies, we arrive at strong subadditivity (3.19), completing the proof. This proof is sketched as pictures in Fig. 3.3. Similar proofs can be constructed for many other inequalities for entanglement entropy and related quantities [97, 98].

As discussed in Section 2.3, vacuum states in QFTs typically follow the area law. We also mentioned that the area law can be violated by nonlocality of the underlying QFT. The area law arises elegantly from geometry in the RT-proposal (3.16) via a volume divergence originating from near the boundary on which we are required to anchor our minimal surfaces. The area law thus seems quite generic in the AdS/CFT correspondence and one might wonder how area law violations would arise in the

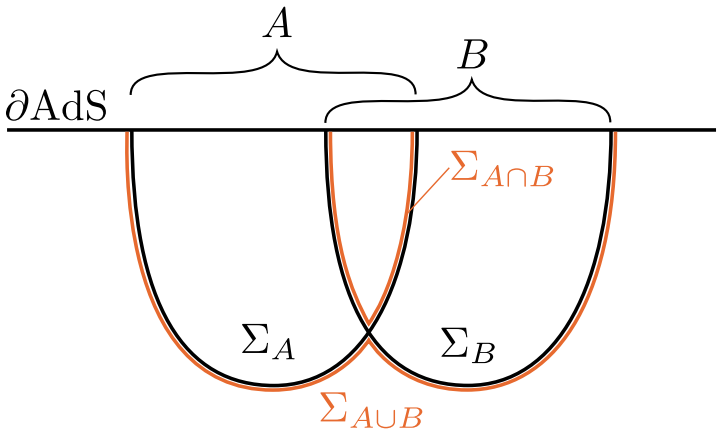

Figure 3.3: Pictorial proof of holographic strong subadditivity. The proof works by rearranging the bulk surfaces Σ_A and Σ_B to $\Sigma_{A\cup B}$ and $\Sigma_{A\cap B}$. This rearrangement preserves the total area, as stated in (3.22). While Σ_A and Σ_B are minimal surfaces by assumption, $\Sigma_{A\cup B}$ and $\Sigma_{A\cap B}$ are not, which completes the proof (3.23). This example shows that in holography, nontrivial properties of entanglement entropy can be inferred by simply drawing the corresponding minimal surfaces.

holographic context. Holographic entanglement entropy can indeed violate the area law if the dual QFT is nonlocal, for example, in noncommutative QFTs [99–101]. In theories with Lorentz symmetry it is expected for the entanglement entropy to satisfy an area law, if we exclude theories with pathological properties [99]. Until now we have mainly discussed asymptotically AdS bulk geometries, where the asymptotic AdS reflects a CFT fixed point in the UV. Noncommutative QFTs evade the area law by being nonlocal. Noncommutativity violates Lorentz symmetry and corresponds to a bulk geometry which is not asymptotically AdS. No longer having an AdS boundary can affect the asymptotic behaviour of minimal surfaces in unusual ways, which can in particular lead to violations of the area law. Noncommutativity of the QFT causes many observables to behave in surprising ways, an example of which can be found in the included paper [III]. Notice though that simply violating Lorentz symmetry does not necessarily produce a violation of the area law [102].

Even in local Lorentz invariant theories, the UV-behaviour (2.49) does not tell the whole story if the entangling region under study contains sharp corners. The presence of corners produces logarithmic terms in addition to the usual area law [I, 103–107].

The formula for holographic entanglement entropy we have discussed here is an approximation since we are working in the limit $N, \lambda \to \infty$ in the QFT. The RT-prescription gives the entanglement entropy of ρ_A up to order N^2 in the number of colours in the QFT. One can consider correcting the RT-formula with either quantum or stringy corrections. Quantum corrections can be considered with the similar treatment as described above, except instead of using the replica trick to compute bulk partition function in the classical approximation, one can compute it in principle to any order in G_N. This will take into account quantum effects in the bulk. The first correction at order G_N^0 or N^0, is

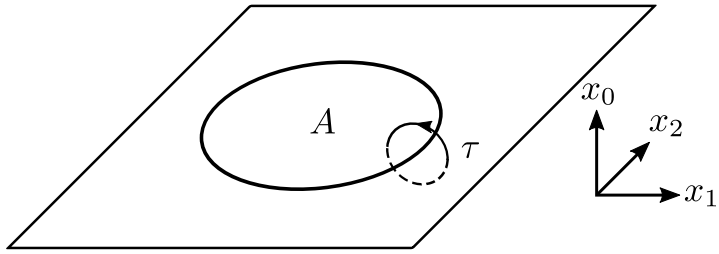

Figure 3.4: The replica trick setup for computing the entanglement entropy of a spherical region. The region A is located at a constant time slice in an Euclidean space and the angular coordinate τ indicates the winding around the entangling surface ∂A which takes one to the next replica copy.

essentially given by the quantum entanglement of the bulk between the different sides of the classical minimal surface [108, 109]. For stringy corrections one needs to consider gravity theories with higher curvature terms. In this case the RT-proposal needs to be generalized to contain corrections involving the extrinsic curvature of the surface [110, 111].

3.2.1 Derivation of the proposal

In this section we shortly outline a derivation of the RT-proposal following [112]. In quantum field theory, the entanglement entropy can be computed, at least in principle, with the replica trick. Our strategy is to extend this method to the holographic context in order to recover the RT-formula.

First, we briefly recall how the replica trick works in field theory. Our setup is illustrated in Fig. 3.4. The goal is to first compute the Rényi entropy

$$S^{(q)}(A) = \frac{1}{1-q} \log \mathrm{tr}_A \left(\rho_A^q\right) \ , \tag{3.24}$$

where $A \subset \mathcal{B}$ is the region we want to find the entanglement entropy of, and ρ_A is the associated reduced density matrix. The Rényi entropy is typically defined for positive integer q, but in our treatment we analytically continue the definition to positive real numbers. The Rényi entropy can be used to find the von Neumann entropy, which for us is the quantity of primary interest

$$S(A) = \lim_{q \to 1} S^{(q)}(A) \ . \tag{3.25}$$

We are now considering static states and pass to Euclidean space. Let us construct a replica manifold $\mathcal{B}_q$ in the following way. We take q copies of the original manifold and glue the copies together at the entangling surface in such a way that encircling the entangling surface takes us from one copy to the next. Furthermore, going around the entangling surface q times takes one back to the original copy. This procedure results in a deficit angle $2\pi(1-q)$ located at ∂A. The Rényi entropy is found by computing the path integral on this q-sheeted surface

$$S^{(q)}(A) = \frac{1}{1-q} \log \frac{Z[\mathcal{B}_q]}{Z[\mathcal{B}]^q} \ . \tag{3.26}$$

The path integral is in general very difficult to compute, but in simple cases the integral can be carried out explicitly [68].

Now we consider the holographic analogue of the above. This time the entangling region lies on the boundary of the spacetime $\partial\mathcal{M} = \mathcal{B}$. The replica manifold is again constructed by taking q copies of $\mathcal{M}$ and gluing them together at ∂A. The boundary of this branched cover of the bulk $\mathcal{M}_q$ should match $\mathcal{B}_q$. The crucial point is that the singular locus at ∂A is assumed to extend into the bulk, forming a bulk codimension-2 surface Σ_A. Since we are working in the holographic dual of the boundary field theory, we can use the bulk partition function to compute (3.26)

$$S^{(q)}(A) = \frac{1}{1-q} \log \frac{Z[\mathcal{M}_q]}{Z[\mathcal{M}]^q} \ . \tag{3.27}$$

This calls for the evaluation of the full string theory partition function. We simplify the problem by working in the classical limit in the bulk. The partition function is then given in the saddle point approximation by the on-shell action

$$\log Z[\mathcal{M}_q] \approx -S_E[\mathcal{M}_q] \ , \tag{3.28}$$

where $\mathcal{M}_q$ solves the equations of motion with the boundary condition $\partial\mathcal{M}_q = \mathcal{B}_q$. The authors of [112] show that in the limit $q \to 1$, receives contributions only from the codimension-2 surface Σ_A, and evaluates to

$$S(A) = \lim_{q\to 1} S^{(q)}(A) = \frac{Vol(\Sigma_A)}{4G_N^{(d+1)}} \ , \tag{3.29}$$

when we work with a $(d+1)$-dimensional bulk and Einstein gravity.

Equation (3.29) already looks a lot like the RT-formula but we still need Σ_A to be a minimal surface. Remarkably, analysing the metric near Σ_A, it can be shown that the equations of motion imply that the traces of the extrinsic curvature matrix vanish in the directions transverse to the surface. The equations for the vanishing of traces of extrinsic curvature coincide with the conditions of a surface to have minimal area. In other words, the entanglement entropy $S(A)$ is calculated by the area of a minimal codimension-2 surface in the bulk, anchored on ∂A on the boundary.

Derivations have also been developed in the time-dependent case which reproduces the HRT-prescription [113]. Extensions to higher derivative gravity also exist [110, 111, 114].

3.2.2 Minimal surfaces

The holographic entanglement entropy proposal calls for the determination of a bulk surface that simultaneously satisfies the correct boundary conditions and has minimal area. We will now outline the way to compute such minimal surfaces and give two explicit examples. We will focus on static spacetimes foliated by constant time hypersurfaces since this simplifies the discussion and is the situation we work in all of the included papers. We start with two pieces of information, the boundary entangling surface ∂A and the bulk metric. The entangling surface provides the boundary condition

that the bulk surface we are trying to find needs to be anchored to ∂A. The bulk metric on the other hand provides the local data necessary to minimize surface areas in the bulk.

Our starting point is the RT-formula

$$S(A) = \frac{1}{4G_N^{(d+1)}} \min_{\Sigma_A} Vol(\Sigma_A) \ . \tag{3.30}$$

Say we have coordinates x in the bulk and coordinates y on the surface, Σ_A, the area of which we are minimizing. The surface Σ_A is embedded in the bulk by some function $f : \Sigma_A \mapsto M$. First we need to find the metric on Σ_A since this quantity contains the information about local geometry necessary for area determination. The metric h on Σ_A is induced by the bulk metric g

$$h = f^* g \tag{3.31}$$

$$= \frac{\partial x^\alpha}{\partial y^\mu} \frac{\partial x^\beta}{\partial y^\nu} g_{\alpha\beta} dy^\mu \otimes dy^\nu \ . \tag{3.32}$$

The area of Σ_A is given by integrating its volume form

$$Vol(\Sigma_A) = \int \sqrt{\det h}\ dy^1 \wedge \cdots \wedge dy^{d-1} \tag{3.33}$$

$$= \int L(x(y), y) dy \ , \tag{3.34}$$

where in the last line we have introduced a "Lagrangian" which depends on the coordinates y on Σ_A and the embeddings $x(y)$. Now one can minimize the area of Σ_A with the same methods one would use to minimize an action integral in a classical mechanics course, that is, we need to solve the Euler-Lagrange equation

$$\frac{\partial}{\partial y^\nu} \left(\frac{\partial L}{\partial(\partial_\nu x^\mu(y))} \right) - \frac{\partial L}{\partial x^\mu(y)} = 0 \ , \tag{3.35}$$

subject to the constraint that Σ_A approaches ∂A near the AdS boundary. Once such a solution is found, it can be plugged back into the integral (3.34) to obtain the volume of Σ_A, and thus also the entanglement entropy $S(A)$. The area is divergent because the boundary on which Σ_A is anchored lies infinitely far away. This divergence is usually regulated by introducing an UV-cutoff so that Σ_A instead of reaching all the way to the boundary of AdS, the surface ends at some $z = \epsilon$. Another way to deal with the divergence is to consider a finite combination of entanglement entropies instead of $S(A)$ itself. One example would be to calculate the difference of entropies between two bulk surfaces with the same boundary conditions. In this way the boundary contributions cancel and the UV-divergence vanishes. One could also study an UV-finite quantity like the mutual information which is discussed in Section 3.4.

Solving the Euler-Lagrange equations for the minimal surface is very difficult in general. In practice, it is a popular choice to restrict one's attention to situations where symmetries can be exploited in such a way that only ordinary differential equations need to be solved. In simple cases one can express the embedding of Σ_A with only one nontrivial embedding function in terms of one coordinate on

Σ_A. One example of this would be a spherical entangling region, in a background with rotational symmetry. Then one can specify the embedding by one function, the boundary radial coordinate as a function of the bulk holographic coordinate. This is an example of a technique where one numerically integrates from the deepest point on Σ_A in the bulk, commonly termed the turning point, toward the boundary to determine the relationship between this turning point and the boundary condition, in this case the radius of A. This integration additionally gives the profile of the minimal surface, which can be used for integrating the minimal area. These types of methods are popular because the numerics required are relatively simple to implement and in some particularly simple cases, for example in pure AdS spaces, some entangling region shapes can be dealt with analytically. We will give two examples of minimal surface calculations shortly.

In cases where symmetries cannot be used for reducing the partial differential equations governing the minimal surface to ordinary differential equations, more complicated numerical methods are required. This may take the form of developing specialized numerical schemes for the specific situation under consideration or using existing numerical software [115, 116].

3.2.3 Examples

In order to give a better feel about how holographic entanglement calculations are done, we briefly go over two example calculations corresponding to the two most common entangling surface shapes in the simplest case of pure AdS_{d+1}, dual to a CFT in d spacetime dimensions [94].

Slab

We choose to express the bulk geometry in Poincaré coordinates (3.15), in which the metric takes the form

$$g = \frac{L^2}{z^2}\left(-dt^2 + dz^2 + d\vec{x}^2\right) \ . \tag{3.36}$$

Here $(t, \vec{x})$ are coordinates on the d-dimensional boundary and z is the holographic coordinate such that $z = 0$ corresponds to the AdS boundary and $z \to \infty$ corresponds to the Poincaré horizon.

If we denote the spatial coordinates of the field theory by $\vec{x} = (x, \vec{x}_\perp)$, a slab of width l is described by a finite interval $-l/2 \leq x \leq l/2$ with the transverse coordinates $\vec{x}_\perp$ being covered by the slab. We consider a spacelike slice of constant time and parametrize the minimal bulk surface by $x = x(z)$. The functional to minimize is

$$S(A) = \frac{L^{d-1}V}{2G_N^{(d+1)}} \int_0^{z_*} \frac{1}{z^{d-1}} \sqrt{1 + x'(z)^2} dz \ , \tag{3.37}$$

where $V = \int d\vec{x}_\perp$ is the volume of the transverse directions and $z = z_*$ is the turning point of the minimal surface, as indicated in Fig. 3.5.

It is generally important to take advantage of symmetries when finding minimal surfaces. Naively, one would find the equation of motion for $x(z)$ by the Euler-Lagrange equation associated with the area functional but then one would end up with a second-order nonlinear differential equation.

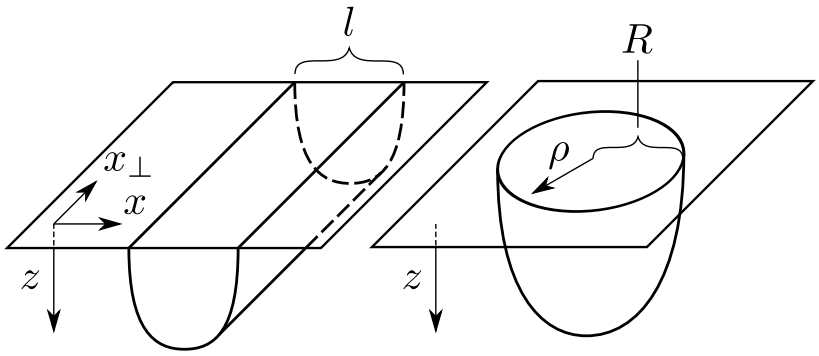

Figure 3.5: Sketches of the RT surfaces for a slab (left) and a sphere (right). The slab has width l along the x-coordinate on the boundary, and extends infinitely in the other spatial boundary dimensions. This removes any edge effects associated to finite length slabs and enables us to describe the bulk profile with a single function $x(z)$. The sphere has radius R and due to rotational symmetry, its bulk profile can also be described with a single function $\rho(z)$.

Translational symmetry $x \to x+a$ is manifest in this simple situation and is reflected by the fact that the area functional depends on $x(z)$ only through its derivatives, which in turn implies that

$$\frac{\partial}{\partial x'(z)} \frac{\sqrt{1+x'(z)^2}}{z^{d-1}} \tag{3.38}$$

is independent of z as a consequence of Euler-Lagrange equations. The value of this constant of motion can be evaluated at the turning point, and used to algebraically solve for $x'(z)$. There are two solutions for $x'(z)$ corresponding to the two branches of the minimal surface starting at the turning point and extending towards the boundary. Here, we have chosen the branch in such a way that $x'(z) \geq 0$. Now knowing the profile of the minimal surface, rest can be solved simply by evaluating two integrals. First, the relation between the slab width l and the turning point z_* is

$$l = \int_{-l/2}^{l/2} dx = 2\int_0^{z_*} x'(z)dz = 2z_* \frac{\sqrt{\pi}\Gamma\left(\frac{d}{2(d-1)}\right)}{\Gamma\left(\frac{1}{2(d-1)}\right)} \,. \tag{3.39}$$

The entanglement entropy is found by plugging $x'(z)$ into the functional, resulting in

$$S(A) = \frac{L^{d-1}V}{2G_N^{(d+1)}} z_*^{2-d} \int_0^1 \frac{d\lambda}{\lambda^{d-1}} \frac{1}{\sqrt{1-\lambda^{2(d-1)}}} \,, \tag{3.40}$$

where we have defined $\lambda = z/z_*$. An important feature of the integral is that there is a divergence originating from the boundary $\lambda = 0$. The divergence corresponds to the expected UV-divergence of the entanglement entropy originating from strong correlations just across the entangling surface. By

separating the divergent and finite parts, we find the entanglement entropy of a slab

$$S(A) = \frac{L^{d-1}}{2(d-2)G_N^{(d+1)}} \left(\frac{V}{\epsilon^{d-2}} - 2^{d-2}\pi^{(d-1)/2} \left(\frac{\Gamma\left(\frac{d}{2(d-1)}\right)}{\Gamma\left(\frac{1}{2(d-1)}\right)} \right)^2 \frac{V}{l^{d-2}} \right) . \tag{3.41}$$

The first term is the famous area law divergence, as can be seen by remembering that the entangling surface volume is $2V$.

Sphere

Now we will calculate the entanglement entropy of a spherical region of radius R in a d-dimensional CFT. Whereas in the case of a slab, the need for solving differential equations was avoided by the use of translation symmetry, we now will exploit the dilatation symmetry to achieve a similar simplification. Adopting spherical coordinates on the boundary, the bulk metric reads

$$g = \frac{L^2}{z^2}\left(-dt^2 + dz^2 + d\rho^2 + \rho^2 d\Omega_{d-2}^2\right) . \tag{3.42}$$

The functional to minimize is then

$$\frac{L^{d-1}V}{4G_N^{(d+1)}} \int_0^{z_*} \frac{\rho^{d-2}}{z^{d-1}} \sqrt{1+\rho'(z)^2} dz . \tag{3.43}$$

The important difference to the slab is that in that case a first integral of (3.37) was easily found due to the cyclic coordinate $x(z)$, but (3.43) has no cyclic coordinates.

Still we can find a conserved quantity via a coordinate transformation [I]. Dilatation symmetry of the background is generated by the Killing vector $k_D = (t, z, \rho, \vec{0})/L$. The integral curves of this isometry are such that the coordinates (t, z, ρ) are multiplied by $e^{\lambda/L}$ for $\lambda \in \mathbb{R}$. The simplifying transformation is to find coordinates in which this dilatation is realized simply as a coordinate translation. In other words, we wish to find coordinates in which the Killing vector becomes $k_D = (0, 0, 1, \vec{0})$. The desired transformation is

$$(t, z, \rho) \to (\tilde{t}, \tilde{z}, u) = \left(\frac{t}{\rho}, \frac{z}{\rho}, \log \frac{\rho}{L} \right) , \tag{3.44}$$

with the identity transformation acting on the coordinates on the S^{d-2}. Note that $\tilde{t}$ and $\tilde{z}$ are invariant under dilatations, while u transforms as $u \mapsto u + \lambda/L$. In the new coordinates, the bulk metric no longer depends on the u-coordinate, reflecting a translational symmetry. The entropy functional, in parametrization $\tilde{z} = \tilde{z}(u)$, is

$$S(A) = \frac{L^{d-1}V}{4G_N^{(d+1)}} \int_0^{\infty} \frac{1}{\tilde{z}(u)^{d-1}} \sqrt{1 + (\tilde{z}(u) + \tilde{z}'(u))^2} du . \tag{3.45}$$

This new functional clearly has a conserved energy associated with u-translations. The rest of the calculation can be done in a manner analogous to slabs. The conserved energy is used to algebraically solve the surface profile $\tilde{z}'(u)$, which can be used to integrate all remaining quantities [I, 116].

3.3 Entanglement wedge

The reduced density matrix ρ_A associated with a region A in the dual QFT contains all information we can have about observables in A. Holographic duality states that the full state ρ of the QFT is dual to all of the bulk spacetime. A natural question arises: which part of the bulk is dual to the reduced density matrix ρ_A? In other words, given ρ_A, we could consider all compatible density matrices ρ on the full state which reduce to ρ_A upon tracing out A^c. Each ρ corresponds to a different bulk, but is there a subregion of the bulk which can be reconstructed with the information contained in ρ_A? The bulk region associated to ρ_A is called the *entanglement wedge* [117–119]. We will now describe the entanglement wedge in more detail.

The reduced density matrix contains the information necessary for computing the entanglement entropy of the region. The bulk dual is a codimension-2 surface hanging in the bulk, anchored on ∂A at the boundary. This extremal surface, Σ, along with the bulk causal structure can be used to split the bulk, $\mathcal{M}$, into four parts.

$$\mathcal{M} = \mathcal{W}_\Sigma(A) \cup \mathcal{W}_\Sigma(A^c) \cup \tilde{J}^+(\Sigma) \cup \tilde{J}^-(\Sigma) \ , \tag{3.46}$$

where $\tilde{J}^+(\Sigma)$ and $\tilde{J}^-(\Sigma)$ are the future and past of Σ, respectively. That is, $\tilde{J}^+(\Sigma)$ is the set of points connectable to Σ by causal future directed curves starting on Σ. The remaining regions, $\mathcal{W}_\Sigma(A)$ and $\mathcal{W}_\Sigma(A^c)$ are the entanglement wedges associated to A and A^c, respectively. To see more clearly where the wedges lie, remember that Σ defines a codimension-1 cohomology surface, $\mathcal{R}_A$, which is bounded by the extremal surface Σ and the boundary entangling region A. The entanglement wedge is the bulk domain of dependence of $\mathcal{R}_A$,

$$\mathcal{W}_\Sigma(A) = \tilde{D}(\mathcal{R}_A) \ . \tag{3.47}$$

Even though any bulk codimension-2 surface could be used for this construction, the extremal surface is special because it is determined by gravitational dynamics of the bulk. For more discussion, see [119].

It is not uncommon for spacetimes to have regions which cannot be probed by extremal surfaces anchored on the boundary [120–122]. These regions are called *entanglement shadows*. A simple example of an entanglement shadow occurs in the case of a nonrotating BTZ black hole. A BTZ black hole is a black hole in $2+1$ spacetime dimension with an asymptotically AdS_3 geometry. It can be thought of as a lower dimensional and asymptotically AdS analogue of the familiar Schwarzschild black hole. A BTZ black hole along with some minimal surfaces is shown in Fig. 3.6. A finite region near the horizon is left untouched by extremal surfaces regardless of the entangling region size. Even though no extremal surface can touch these shadow regions, entanglement shadows are reconstructible using the information contained in boundary density matrices because the shadow regions are contained in either the entanglement wedge of A or A^c.

Finding the bulk region dual to a boundary reduced density matrix is a part of a larger subject of bulk reconstruction. In general, it should be possible to infer the structure of the bulk completely just by studying QFT observables. It is possible to reconstruct static, spherically symmetric, and

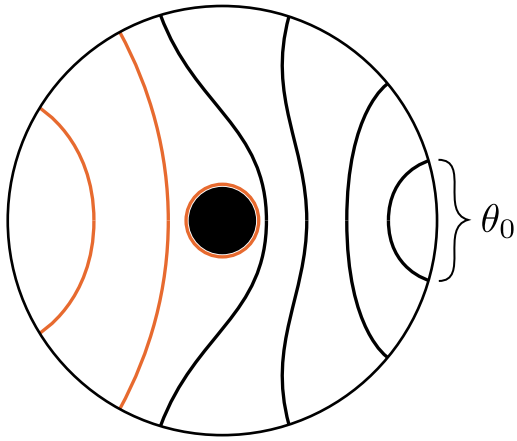

Figure 3.6: A BTZ-black hole geometry and some minimal surfaces. The boundary is a circle and the entangling regions are intervals of width θ_0. For sufficiently thin surfaces (black curves), the minimal surfaces are simply connected. If θ_0 is large enough (orange curves), the minimal surfaces are composed of two parts: one part that reaches the boundary and one part that wraps the black hole horizon. An entanglement shadow exists, because there is a region of finite size around the black hole horizon which is never touched by any minimal surface. The minimal surfaces approach the horizon when θ_0 is increased, but they cannot reach arbitrarily close to the horizon because for some θ_0 the minimal surfaces become an union of the horizon and a surface finite distance away from the horizon.

asymptotically AdS spacetimes using geodesics and entanglement entropy [123–127]. Subsequently it has been shown that even general metrics can be uniquely fixed by the knowledge of boundary entanglement entropy of differently shaped regions [128, 129]. For more on the relation between entanglement and bulk geometry one should see [130–134]. Bulk fields can be given in terms of boundary operators by first solving the bulk equations of motion [135–140]. These bulk operator reconstructions are possible in the entanglement wedge as was proved in [141]. More general bulk geometric objects can be constructed with boundary entanglement entropy: spacelike curves [142] and further, general bulk surfaces can be reconstructed with differential entropy [143–146]. In a similar vein, progress has been made towards extracting the dynamics of the bulk from entanglement [147–149].

3.4 Mutual information

The entanglement entropy in QFT contains an UV-divergence originating from strong short range correlations across the entangling surface. This divergence is reflected in the holographic computation of entanglement entropy via the infinite volume of the RT-surface. In actual calculations the divergence has to be regulated somehow which has the downside of making results dependent on the regularization scheme. The benefit in studying mutual information is that it gives a finite and thus

regularization scheme independent correlation measure. Its definition has been discussed in Section 2.2. For two disjoint regions A and B, the mutual information denoted by $I(A,B)$ is

$$I(A,B) = S(A) + S(B) - S(AB) \ . \tag{3.48}$$

UV-finiteness of the combination can be seen by noting that divergences of each term originate from the part of the RT-surface near the boundary. Each near boundary part is counted once with positive sign and once with a negative sign, $\partial A \cup \partial B = \partial(A \cup B)$, cancelling out the divergences. Nonnegativity of $I(A,B)$ follows from subadditivity [96], with equality $I(A,B) = 0$ occurring when the RT-surface corresponding to AB is an union of two disjoint bulk surfaces, one being the same as the RT-surface of region A alone and similarly for B. This vanishing usually happens when the distance between A and B is much larger than their individual sizes. An example of this interplay between competing locally minimal surfaces is shown in Fig. 3.7. Further, mutual information increases monotonically when adding parts to A or B

$$I(A,BC) \geq I(A,B) \ , \tag{3.49}$$

in accordance with the intuition that it should measure the total amount of correlation between subsystems.

We can also measure quantum information with conditional entanglement measures. *Conditional entanglement entropy* measures the amount of uncertainty about a spatial region A conditioned on the knowledge about an another region B

$$H(A|B) = S(AB) - S(B) \ . \tag{3.50}$$

Subadditivity of entanglement entropy (2.36) guarantees that $S(A) \geq H(A|B)$. This means that knowledge about a region B cannot increase our uncertainty about region A, exactly like in the classical case with conditional Shannon entropy (2.9). A striking difference to the classical case is that in the quantum case $H(A|B)$ can be negative, meaning that sometimes one can be more certain about the composite system ρ_{AB} than about its constituents. This is a fundamental property of quantum entanglement and can be seen to occur even in the simplest case of two qubits in a Bell state.

An analogous conditioned version can be defined for the mutual information,

$$I(A,B|C) = S(AB) + S(BC) - S(C) - S(ABC) \ . \tag{3.51}$$

The conditional mutual information $I(A,B|C)$ is guaranteed to be nonnegative by strong subadditivity of entanglement entropy (2.35). As usual, conditional mutual information has the advantage of UV-finiteness over conditional entanglement entropy.

Holographic mutual information satisfies the following tripartite inequality

$$I(A,B) + I(A,C) \leq I(A,BC) \ , \tag{3.52}$$

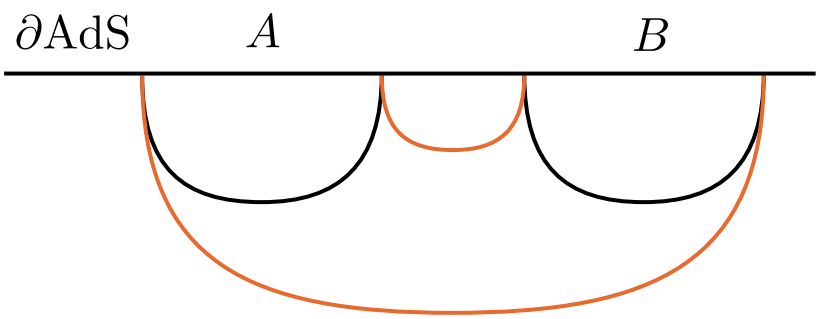

Figure 3.7: Competing phases for the mutual information of two parallel slabs. When the slabs A and B are sufficiently far away from each other, the disconnected phase is dominant (black surfaces). The disconnected phase corresponds to vanishing mutual information. If the slabs are brought closer together, there is a point when the connected (orange) surfaces have the minimal area. The connected phase signals that A and B have nonvanishing mutual information.

for all disjoint regions A, B, and C [97]. This property is called *monogamy* of holographic mutual information and it is symmetric under permutations of A, B, and C, which can be seen by expanding all terms using the definition of $I(A,B)$ in terms of the entanglement entropy. Monogamy can be seen as a statement about the extensivity of mutual information [II]. In the case where the inequality saturates, the mutual information of A with BC would be equal to the mutual information of A with B and C separately. In this way the shared information increases extensively: when combining B and C, the mutual information is simply a sum of individual amounts of mutual information. Typically though, the inequality does not saturate in which case we say that mutual information is superextensive. That is, A has more mutual information with BC than it has with the parts B and C individually. We have introduced a quantity to characterize the degree of extensivity of mutual information

$$e = \frac{I(A,BC)}{I(A,B)+I(A,C)} \,, \tag{3.53}$$

which we simply call *extensivity* [II]. The mutual information in a theory behaves superextensively if $e>1$, subextensively if $0<e<1$, and exactly extensively if $e=1$.

The monogamy of mutual information is a special property of field theories with holographic duals, since there are simple examples of quantum states where monogamy is violated [97]. One way to view (3.52) is that it gives a necessary condition for a field theory to have a dual gravitational description via holography.

In general quantum systems, correlations between operators in two subsystems A and B are bounded from above by their mutual information $I(A,B)$ [150]

$$I(A,B) \geq \frac{\mathcal{C}(M_A,M_B)^2}{2\|M_A\|^2\|M_B\|^2} \,, \tag{3.54}$$

where $\mathcal{C}(M_A, M_B) = \langle M_A \otimes M_B \rangle - \langle M_A \rangle \langle M_B \rangle$ measures correlations of observables M_A and M_B. This inequality tells us that if we have two subsystems with a vanishing mutual information, the subsystems cannot have correlations in any observables. It is common for the mutual information to undergo phase transitions between competing minimal surfaces in the bulk, such as the one shown in Fig. 3.7. Generally, there exists a phase where $I(A, B) = 0$, which can be realized by taking the sizes of A and B to be small when compared to their separation. The calculation of correlation functions in AdS/CFT is not covered in this thesis but good explanations of the subject can be found, for example, in [151].

In the situation depicted in Fig. 3.7, entanglement entropy has only two phases, corresponding to the two competing bulk minimal surfaces anchored to $\partial(AB)$. Different gravitational backgrounds can have a richer phase structure, however. For example, in confining backgrounds where the bulk space ends at some $z = z_0$, where z is the radial coordinate in the Poincaré patch (3.15). In this case more competing bulk surfaces appear, namely, disconnected surfaces which dive straight down from the boundary $z = 0$ to the point where the space ends at $z = z_0$. Another way to have more complex phase structure is to consider more than two spatial regions, or regions that are composed of disconnected parts [I, 152].

3.5 Entanglement wedge cross section

The von Neumann entropy is the unique measure of entanglement between subsystems A and B making up a pure state and a simple bulk dual for it is given by the RT-proposal (3.16). Quantum information theory has multiple quantities for measuring correlations, both classical and quantum, of a system in a mixed state, but not much is known about their bulk duals in holographic theories. As discussed in the previous chapter of this thesis, one such correlation measure is the entanglement of purification, $E_P(A, B)$. Entanglement of purification is of particular interest for us because there is a proposition for its holographic dual [153]. The proposed dual is called the *entanglement wedge cross section*, $E_W(A, B)$.

Consider a static asymptotically AdS_{d+1} spacetime dual to some holographic QFT. We denote the canonical time slice of the bulk by M. On the boundary ∂M, we have two regions A and B with no nonzero overlap. We assume that the entanglement wedge, M_{AB}, associated to AB is connected, and the corresponding minimal surface is Γ_{AB}. In other words, $\partial M_{AB} = A \cup B \cup \Gamma_{AB}$. Next, we split the minimal surface Γ_{AB} into two parts

$$\Gamma_{AB} = \Gamma_{AB}^{(A)} \cup \Gamma_{AB}^{(B)} \, . \tag{3.55}$$

There are infinitely many ways of splitting Γ_{AB} into two parts, reflecting the infinite number of ways one can purify a mixed state. Further, we define

$$\tilde{\Gamma}_A = A \cup \Gamma_{AB}^{(A)} \tag{3.56}$$

$$\tilde{\Gamma}_B = B \cup \Gamma_{AB}^{(B)} \, . \tag{3.57}$$

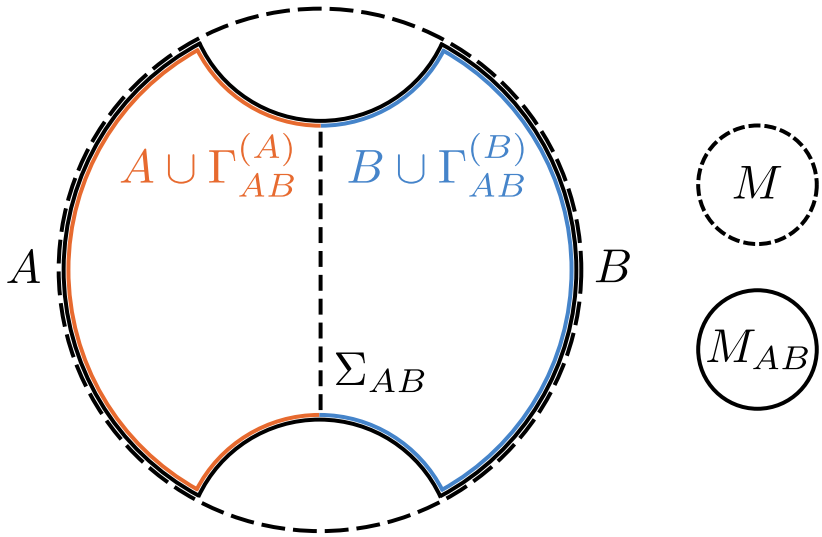

Figure 3.8: Our setup for the definition of the entanglement wedge cross section E_W. The diagram represents a time slice of an asymptotically AdS_{d+1} spacetime M. The black dashed circle represents the boundary ∂M on which the QFT lives. The solid black curve outlines the entanglement wedge M_{AB}, assuming that the regions A and B are such that the entanglement wedge is connected. The coloured lines visualize a partition of the entanglement wedge boundary, as in (3.59). The dashed line is the surface Σ_{AB}, which divides M_{AB} into two parts. The entanglement wedge cross section is given in terms of this surface, as in (3.61).

The point is that $\tilde{\Gamma}_A$ and $\tilde{\Gamma}_B$ give together us a new partition of the entanglement wedge boundary

$$\partial M_{AB} = A \cup B \cup \Gamma_{AB} \tag{3.58}$$
$$= A \cup \Gamma_{AB}^{(A)} \cup B \cup \Gamma_{AB}^{(B)} \tag{3.59}$$
$$= \tilde{\Gamma}_A \cup \tilde{\Gamma}_B \ , \tag{3.60}$$

in such a way that $A \subset \tilde{\Gamma}_A$ and $B \subset \tilde{\Gamma}_B$. See Fig. 3.8 for a visualization of these surfaces.

Now we are in a position to define the surface we need for the definition of $E_W(A, B)$. Let Σ_{AB} be a bulk surface which

(i) is anchored on $\tilde{\Gamma}_{A,B}$: $\partial\Sigma_{AB} = \partial\tilde{\Gamma}_A = \partial\tilde{\Gamma}_B$

(ii) is homologous to $\tilde{\Gamma}_A$ inside M_{AB} .

The surface Σ_{AB} has the property of dividing the entanglement wedge into two parts in such a way that one part contains A and the other contains B. The conditions above still do not uniquely determine Σ_{AB}, since there exist many surfaces anchored on $\tilde{\Gamma}_A$ and further, many different splits of Γ_{AB} in (3.55). The entanglement wedge cross section is defined by minimizing the area of Σ_{AB} for

a given split of Γ_{AB} and then finding the split with minimal $Vol(\Sigma_{AB})$,

$$E_W(A,B) = \min_{\tilde{\Gamma}_{A,B}} \min_{\Sigma_{AB}:\partial\Sigma_{AB}=\partial\tilde{\Gamma}_A} \frac{Vol(\Sigma_{AB})}{4G_N^{(d+1)}} \ . \tag{3.61}$$

Now we see that $E_W(A,B)$ is understood to give the smallest possible area of a surface that splits the entanglement wedge into a part associated with A and a part associated with B. Given that a disconnected entanglement wedge signals the absence of correlation between A and B, it seems natural to assume that the size, as measured by the minimal cross section, of the entanglement wedge connecting A and B could give a measure of correlation. The entanglement wedge cross section is the natural quantity for measuring the correlations represented by a connected entanglement wedge.

This construction is natural when thought of in light of the surface-state correspondence [154–157]. The mixed state ρ_{AB} corresponds to $A\cup B$ and the traced out part of the boundary is pulled into the bulk until the surface becomes extremal, which corresponds to some quantum state R. The union of A, B, and R is a closed convex surface in the sense of [154] and corresponds to a pure state $|ABR\rangle$, which is a purification of ρ_{AB}. Now the prescription for computing E_W seems more natural: ∂M_{AB} is dual to a purification of ρ_{AB}, which is then split in such a way that the entanglement of $A\cup\Gamma_{AB}^{(A)}$ is minimal, analogously to the definition of E_P (2.45).

As an entanglement measure of mixed states, $E_W(A,B)$ satisfies many important properties that are clear by considering Σ_{AB} in different cases. Firstly, $E_W(A,B)\geq 0$ for all ρ_{AB} because the volume of Σ_{AB} can only be nonnegative. Secondly, E_W vanishes trivially for product states $\rho_{AB}=\rho_A\otimes\rho_B$ because they correspond to disconnected entanglement wedges because of $I(A,B)=0$. Thirdly, if ρ_{AB} is a pure state, $E_W(A,B)$ reduces to the entanglement entropy of ρ_A. This can be seen by noting that for pure ρ_{AB}, the minimal surface $\Gamma_{AB}=\emptyset$, reducing $\tilde{\Gamma}_A$ to A. Then the split minimization of (3.61) becomes trivial with boundary conditions $\partial\Sigma_{AB}=\partial A=\partial B$ thus reducing $E_W(A,B)$ to $S(A)$. More nontrivially, the entanglement wedge cross section satisfies

$$E_W(A,B)\geq\frac{I(A,B)}{2} \ , \tag{3.62}$$

as is required if $E_W(A,B)$ is to give the bulk dual of $E_P(A,B)$ [29]. The holographic proof of this inequality is sketched in Fig. 3.9.

Calculations of E_W are in principle straightforward but in practice requires the use of nontrivial numerical schemes. Analytical calculations can be carried out in simple cases where symmetries of the background and entanglement regions immediately imply the shape of Σ_{AB}. As a practical example consider the case of two parallel, infinite slabs in the Poincaré patch of AdS. The possible bulk surfaces corresponding to the entanglement entropy of this system are the same ones as are shown in Fig. 3.7. In the connected phase, the entanglement wedge is the region bounded by an U-shaped surface connecting the closer edges of the entanglement regions and an another surface hanging deeper in the bulk, connecting the far edges of the boundary regions. Now, if the boundary slabs have equal width, then by symmetry, the surface Σ_{AB} splitting the entanglement wedge must be a flat surface at a constant x-slice connecting the turning points of the bulk surfaces bounding M_{AB}. Then it is a simple matter to calculate E_W. Indeed, this was one of the first explicit calculations of E_W, first

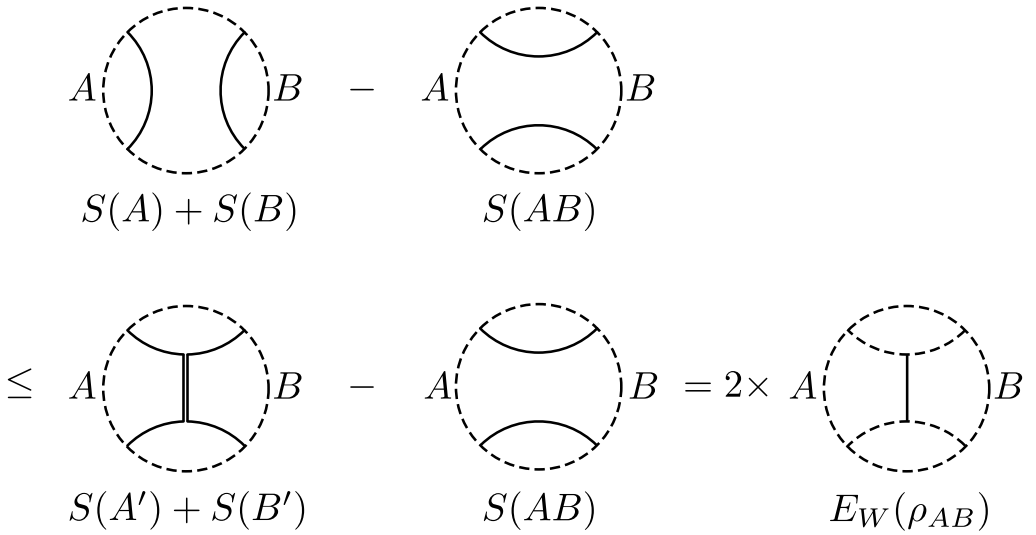

Figure 3.9: A pictorial representation of the proof for the inequality $E_W(A,B) \geq I(A,B)/2$. The dashed circle in each diagram represents the AdS boundary. Solid lines represent bulk surfaces whose areas yield the entanglement entropy terms below the diagrams. The diagrams on the first line represent the computation of $I(A,B)$. On the second line, the bulk surfaces corresponding to A and B are deformed such that their anchor points on the boundary are not changed, but the bulk parts are no longer minimal area surfaces. Finally, subtracting surfaces in the indicated way establishes the inequality (3.62).

in AdS_3 [153] and later in AdS_{d+1} [I]. Now consider the same setup except with slabs of different width. Symmetry is insufficient in this case for identifying the minimal surface for splitting M_{AB} and one has to resort to numerics. Still the computation is relatively simple since one knows a priori that Σ_{AB} must be a segment of a usual bulk surface associated with a boundary slab, but the parameters for characterizing a specific surface must be searched numerically [158].

Chapter 4

Summary

In this introduction we have seen applications of holography to quantum information theory. The goal of quantum information theory is to study the properties and distribution of information in quantum systems. It is, however, exceedingly difficult to compute many quantities of interest in quantum field theories in all but the simplest toy models. We have shown that holography can be used to transform the problem of finding the entanglement entropy to a tractable form in certain interacting quantum field theories. This is accomplished with the Ryu-Takayanagi prescription, which expresses the entanglement entropy in terms of the area of a certain minimal surface. The insight behind gauge/gravity dualities is that in certain strongly interacting quantum field theories, collective excitations give rise to a new weakly coupled description of the same physics. Surprisingly, these weakly coupled dynamics are governed by classical gravity with one more spatial dimension. This way of translating problems in strongly coupled field theories to the language of classical gravity massively simplifies calculations, in particular, enabling the computation of entanglement entropy.

We introduced information theoretical concepts, first classically, then in the context of quantum mechanics, and finally we saw how to use holography in their computation. Most of our work revolved around the entanglement entropy and quantities closely related to it, for example, we covered properties of the mutual information and the entanglement of purification. We showed how the holographic entanglement entropy proposal satisfies the properties that the dual of the von Neumann entropy should satisfy. In particular, the proposal satisfies the famous area law and the way it is realized has an intuitive geometrical interpretation. The entanglement entropy satisfies a number of inequalities, the most important of which we proved for the holographic proposal. Entanglement of purification is an entanglement measure for mixed states. It has been an important quantity in our research, and as such we discussed its holographic dual candidate, the entanglement wedge cross section, in detail.

Entanglement is a fundamental property in quantum mechanics and thus by probing its properties we can learn about the underlying nature of quantum matter. Entanglement quantities have attracted a lot of interest due to their applications in the study of many phenomena, for example, in the thermalization of strongly coupled plasma. This interest is bound to persist in the future.

Glossary

Araki-Lieb inequality

An inequality satisfied by the von Neumann entropy on bipartite quantum states. It highlights the property of quantum entanglement that a composite system can have lower entropy than the entropy of its parts. 14

area law

A behaviour of entanglement entropy common in ground states of local quantum systems where the leading term of the entanglement entropy is proportional to the area of the boundary of the region considered. 18

a-theorem

An analogue of the c-theorem in even dimensions higher than two based on certain trace anomalies. 20

conditional entanglement entropy

A quantum generalization of the classical conditional entropy. Unlike the conditional entropy, the conditional entanglement entropy can be negative. 39

conditional entropy

A measure of uncertainty about a system after learning the state of an another system. The knowledge about the second system cannot increase the amount of uncertainty about the original system. 8

c-theorem

A theorem stating that two-dimensional quantum field theories always have a function $c(g)$ depending on the coupling constants g of the theory such that the function decreases monotonically along the renormalization group flow and becomes stationary at fixed points. At a fixed point of the renormalization group flow, the value of the function is equal to the central charge of the corresponding CFT. 20

density operator

A Hermitian and non-negative linear operator with unit trace describing a quantum state. The density operator gives a description of a quantum state equivalent to the description in terms of state vectors. The terms density operator and density matrix are often used interchangeably. 9

entanglement

A quantum phenomenon where two physical systems cannot be described independently of each other, in the sense that the quantum state does not factor to a product of states of the two systems. The amount of entanglement can be quantified by entanglement measures, a prominent example of which is the entanglement entropy. 11

entanglement of purification

An entanglement measure for mixed states based on first purifying the state and then minimizing the von Neumann entropy over all purifications. The entanglement of purification reduces to the von Neumann entropy in the case of a pure state. 16

entanglement shadow

A bulk region which cannot be probed by any extremal surface anchored on the boundary. 37

entanglement wedge

The bulk region encoding the information contained in a reduced density matrix of the boundary theory. 37

entanglement wedge cross section

A measure of correlations between two subsystems in a QFT with a holographic dual. This entanglement measure is proposed to be the holographic dual of the entanglement of purification. 41

extensivity

A quantity characterizing the behaviour of mutual information between two regions when one of the regions is scaled. 40

F-theorem

An analogue of the c-theorem in three dimensional QFTs. 20

gauge/gravity duality

A holographic duality between a classical theory of gravity and a quantum field theory. The QFT has one spatial dimension less and is said to live on the boundary of the bulk manifold governed by gravity. 2

global coordinates

A coordinate chart that covers the entire anti de-Sitter manifold. 23

holographic principle

A conjecture about quantum gravity stating that $(d+1)$-dimensional quantum gravity states can be naturally described by a theory in d dimensions. The primary example of the holographic principle is the AdS/CFT correspondence. 21

maximally entangled state

A composite state such that the reduced density operators of subsystems are proportional to identity operators. The entanglement entropy takes its largest possible value on maximally entangled states. 11

monogamy of mutual information

An inequality satisfied by quantum states with holographic duals but not generic quantum states. Monogamy states that the holographic mutual information is never a subextensive quantity. 40

mutual information

A measure of the amount of information shared between two systems. The mutual information can be equivalently understood as measuring the amount of information one gains about a system when one learns the state of an another system. 8

Poincaré coordinates

A coordinate chart commonly used for the anti de-Sitter spacetime. In Poincaré coordinates, the metric is proportional to the Minkowski metric and many symmetries of AdS are explicit. 23, 25

Poincaré horizon

The surface which separates the Poincaré patch from the rest of the anti de-Sitter manifold. 26

Poincaré patch

The coordinate patch of AdS covered by the Poincaré coordinates. The Poincaré patch covers the anti de-Sitter spacetime only partially. 26

product state

A composite quantum state that can be written as a product of states on its individual subsystems. A product state has no entanglement. 12

purification of a state

A pure state that can be associated to any mixed state by the introduction of an auxiliary state on an auxiliary Hilbert space. The original state is recovered from the purification by partially tracing over the auxiliary Hilbert space. A purification of a mixed state is not unique. 12

qubit

A quantum version of a classical binary bit. A qubit is realized as a two-level quantum system, for example, the spin of an electron. Instead of taking one of two values like a bit, a qubit can be in any superposition of its two basis states. 11

reduced density matrix

A partial trace of a density matrix. The reduced density matrix is used in a situation where only a subsystem of a composite quantum system is accessible, and as such contains the information needed to calculate the entanglement entropy associated to the subsystem. 11

renormalization group

A mathematical tool which allows the study of a quantum many body system at different length or energy scales. 19

Schmidt decomposition

A particularly simple form in which one always can express a vector in the tensor product space of two Hilbert spaces. 10

Schmidt number

The number of terms in the Schmidt decomposition of a state vector. If the Schmidt number is one, the state is a product state. Otherwise the state is entangled. 12

separable state

A mixed quantum state which can be written as a linear combination of product states. 12

Shannon entropy

A measure of uncertainty about a system in classical information theory. 6

strong subadditivity

A fundamental inequality satisfied by the Shannon and von Neumann entropies. 7, 14

subadditivity

An inequality satisfied by the Shannon and von Neumann entropies. Subadditivity has the interpretation that in a system of two random variables, the uncertainty about the joint system can never exceed the sum of uncertainties about its parts. 7, 14

von Neumann entropy

An entanglement measure on quantum states. It is the quantum analogue of Shannon entropy. The von Neumann entropy is unique on pure composite states. 13

Bibliography

[I] Niko Jokela and Arttu Pönni. "Notes on entanglement wedge cross sections". In: *JHEP* 07 (2019), p. 087. arXiv: 1904.09582 [hep-th].

[II] Vijay Balasubramanian et al. "Information flows in strongly coupled ABJM theory". In: *JHEP* 01 (2019), p. 232. arXiv: 1811.09500 [hep-th].

[III] Yago Bea et al. "Noncommutative massive unquenched ABJM". In: *Int. J. Mod. Phys.* A33.14n15 (2018), p. 1850078. arXiv: 1712.03285 [hep-th].

[IV] Niko Jokela, Arttu Pönni, and Aleksi Vuorinen. "Small black holes in global AdS spacetime". In: *Phys. Rev.* D93.8 (2016), p. 086004. arXiv: 1508.00859 [hep-th].

[1] Blaise Goutéraux, Niko Jokela, and Arttu Pönni. "Incoherent conductivity of holographic charge density waves". In: *JHEP* 07 (2018), p. 004. arXiv: 1803.03089 [hep-th].

[2] P. Kovtun, Dan T. Son, and Andrei O. Starinets. "Viscosity in strongly interacting quantum field theories from black hole physics". In: *Phys. Rev. Lett.* 94 (2005), p. 111601. arXiv: hep-th/0405231 [hep-th].

[3] Juan Martin Maldacena. "The Large N limit of superconformal field theories and supergravity". In: *Int. J. Theor. Phys.* 38 (1999). [Adv. Theor. Math. Phys.2,231(1998)], pp. 1113–1133. arXiv: hep-th/9711200 [hep-th].

[4] Jacob D. Bekenstein. "Black holes and entropy". In: *Phys. Rev.* D7 (1973), pp. 2333–2346.

[5] Gerard 't Hooft. "Dimensional reduction in quantum gravity". In: *Conf. Proc.* C930308 (1993), pp. 284–296. arXiv: gr-qc/9310026 [gr-qc].

[6] Leonard Susskind. "The World as a hologram". In: *J. Math. Phys.* 36 (1995), pp. 6377–6396. arXiv: hep-th/9409089 [hep-th].

[7] Romuald A. Janik. "AdS/CFT and applications". In: *PoS* EPS-HEP2013 (2013), p. 141. arXiv: 1311.3966 [hep-ph].

[8] Jorge Casalderrey-Solana et al. "Gauge/String Duality, Hot QCD and Heavy Ion Collisions". In: (2011). arXiv: 1101.0618 [hep-th].

[9] Subir Sachdev. "What can gauge-gravity duality teach us about condensed matter physics?" In: *Ann. Rev. Condensed Matter Phys.* 3 (2012), pp. 9–33. arXiv: 1108.1197 [cond-mat.str-el].

[10] Andrea Amoretti et al. "A holographic strange metal with slowly fluctuating translational order". In: (2018). arXiv: 1812.08118 [hep-th].

[11] Tatsuma Nishioka, Shinsei Ryu, and Tadashi Takayanagi. "Holographic Entanglement Entropy: An Overview". In: *J. Phys.* A42 (2009), p. 504008. arXiv: 0905.0932 [hep-th].

[12] A. Einstein, B. Podolsky, and N. Rosen. "Can Quantum-Mechanical Description of Physical Reality Be Considered Complete?" In: *Phys. Rev.* 47 (10 May 1935), pp. 777–780. URL: https://link.aps.org/doi/10.1103/PhysRev.47.777.

[13] J. S. Bell. "On the Einstein-Podolsky-Rosen paradox". In: *Physics Physique Fizika* 1 (1964), pp. 195–200.

[14] Alain Aspect, Philippe Grangier, and Gerard Roger. "Experimental Tests of Realistic Local Theories via Bell's Theorem". In: *Phys. Rev. Lett.* 47 (1981), pp. 460–6443.

[15] Alain Aspect, Jean Dalibard, and Gerard Roger. "Experimental test of Bell's inequalities using time varying analyzers". In: *Phys. Rev. Lett.* 49 (1982), pp. 1804–1807.

[16] C. E. Shannon. "A Mathematical Theory of Communication". In: *Bell System Technical Journal* 27.3 (1948), pp. 379–423.

[17] Phillippe H. Eberhard and Ronald R. Ross. "Quantum field theory cannot provide faster-than-light communication". In: *Foundations of Physics Letters* 2.2 (Mar. 1989), pp. 127–149.

[18] Asher Peres and Daniel R. Terno. "Quantum information and relativity theory". In: *Rev. Mod. Phys.* 76 (1 Jan. 2004), pp. 93–123. URL: https://link.aps.org/doi/10.1103/RevModPhys.76.93.

[19] Ryszard Horodecki et al. "Quantum entanglement". In: *Rev. Mod. Phys.* 81 (2 June 2009), pp. 865–942. URL: https://link.aps.org/doi/10.1103/RevModPhys.81.865.

[20] N. Pippenger. "The inequalities of quantum information theory". In: *IEEE TIT* 49.4 (2003).

[21] Elliott H. Lieb and Mary Beth Ruskai. "Proof of the Strong Subadditivity of Quantum-Mechanical Entropy". In: *Les rencontres physiciens-mathématiciens de Strasbourg -RCP25* 19 (1973).

[22] János Aczél, B Forte, and Che Tat Ng. "Why the Shannon and Hartley entropies are 'natural'". In: *Advances in Applied Probability* 6 (Mar. 1974), pp. 131–146.

[23] W. Ochs. "A new axiomatic characterization of the von Neumann entropy". In: *Reports on Mathematical Physics* 8.1 (1975), pp. 109–120. URL: http://www.sciencedirect.com/science/article/pii/0034487775900221.

[24] Josh Cadney, Noah Linden, and Andreas Winter. "Infinitely many constrained inequalities for the von Neumann entropy". In: *IEEE TIT* 58 (2012). arXiv: 1107.0624 [quant-ph].

[25] Kavan Modi et al. "The classical-quantum boundary for correlations: Discord and related measures". In: *Reviews of Modern Physics* 84.4 (Oct. 2012), pp. 1655–1707. arXiv: 1112.6238 [quant-ph].

[26] Berry Groisman, Sandu Popescu, and Andreas Winter. "Quantum, classical, and total amount of correlations in a quantum state". In: *pra* 72.3, 032317 (Sept. 2005), p. 032317. arXiv: quant-ph/0410091 [quant-ph].

[27] Matthew J. Donald, Michał Horodecki, and Oliver Rudolph. "The uniqueness theorem for entanglement measures". In: *Journal of Mathematical Physics* 43.9 (Sept. 2002), pp. 4252–4272. arXiv: quant-ph/0105017 [quant-ph].

[28] Ingemar Bengtsson and Karol Zyczkowski. *Geometry of Quantum States: An Introduction to Quantum Entanglement*. Cambridge University Press, 2006.

[29] Barbara M. Terhal et al. "The entanglement of purification". In: *Journal of Mathematical Physics* 43.9 (Sept. 2002), pp. 4286–4298. arXiv: quant-ph/0202044 [quant-ph].

[30] Shrobona Bagchi and Arun Kumar Pati. "Monogamy, polygamy, and other properties of entanglement of purification". In: *pra* 91.4, 042323 (Apr. 2015), p. 042323. arXiv: 1502.01272 [quant-ph].

[31] W. Dür and H. J. Briegel. "Entanglement purification and quantum error correction". In: *Reports on Progress in Physics* 70.8 (Aug. 2007), pp. 1381–1424. arXiv: 0705.4165 [quant-ph].

[32] P. V. Buividovich and M. I. Polikarpov. "Entanglement entropy in gauge theories and the holographic principle for electric strings". In: *Phys. Lett.* B670 (2008), pp. 141–145. arXiv: 0806.3376 [hep-th].

[33] William Donnelly. "Decomposition of entanglement entropy in lattice gauge theory". In: *Phys. Rev.* D85 (2012), p. 085004. arXiv: 1109.0036 [hep-th].

[34] Horacio Casini, Marina Huerta, and Jose Alejandro Rosabal. "Remarks on entanglement entropy for gauge fields". In: *Phys. Rev.* D89.8 (2014), p. 085012. arXiv: 1312.1183 [hep-th].

[35] William Donnelly. "Entanglement entropy and nonabelian gauge symmetry". In: *Class. Quant. Grav.* 31.21 (2014), p. 214003. arXiv: 1406.7304 [hep-th].

[36] Alexander M. Polyakov. "Gauge Fields and Strings". In: *Contemp. Concepts Phys.* 3 (1987), pp. 1–301.

[37] John Kogut and Leonard Susskind. "Hamiltonian formulation of Wilson's lattice gauge theories". In: *Phys. Rev. D* 11 (2 Jan. 1975), pp. 395–408. URL: https://link.aps.org/doi/10.1103/PhysRevD.11.395.

[38] John B. Kogut. "An introduction to lattice gauge theory and spin systems". In: *Rev. Mod. Phys.* 51 (4 Oct. 1979), pp. 659–713. URL: https://link.aps.org/doi/10.1103/RevModPhys.51.659.

[39] Mark Srednicki. "Entropy and area". In: *Phys. Rev. Lett.* 71 (1993), pp. 666–669. arXiv: hep-th/9303048 [hep-th].

[40] Michael M. Wolf. "Violation of the entropic area law for Fermions". In: *Phys. Rev. Lett.* 96 (2006), p. 010404. arXiv: quant-ph/0503219 [quant-ph].

[41] Dimitri Gioev and Israel Klich. "Entanglement Entropy of Fermions in Any Dimension and the Widom Conjecture". In: *Phys. Rev. Lett.* 96 (2006), p. 100503. arXiv: quant-ph/0504151 [quant-ph].

[42] Noriaki Ogawa, Tadashi Takayanagi, and Tomonori Ugajin. "Holographic Fermi Surfaces and Entanglement Entropy". In: *JHEP* 01 (2012), p. 125. arXiv: 1111.1023 [hep-th].

[43] Noburo Shiba and Tadashi Takayanagi. "Volume Law for the Entanglement Entropy in Non-local QFTs". In: *JHEP* 02 (2014), p. 033. arXiv: 1311.1643 [hep-th].

[44] Wei Li and Tadashi Takayanagi. "Holography and Entanglement in Flat Spacetime". In: *Phys. Rev. Lett.* 106 (2011), p. 141301. arXiv: 1010.3700 [hep-th].

[45] Joanna L. Karczmarek and Philippe Sabella-Garnier. "Entanglement entropy on the fuzzy sphere". In: *JHEP* 03 (2014), p. 129. arXiv: 1310.8345 [hep-th].

[46] Charles Rabideau. "Perturbative entanglement entropy in nonlocal theories". In: *JHEP* 09 (2015), p. 180. arXiv: 1502.03826 [hep-th].

[47] Hong Liu and Mark Mezei. "A Refinement of entanglement entropy and the number of degrees of freedom". In: *JHEP* 04 (2013), p. 162. arXiv: 1202.2070 [hep-th].

[48] H. Casini and M. Huerta. "Analytic results on the geometric entropy for free fields". In: *J. Stat. Mech.* 0801 (2008), P01012. arXiv: 0707.1300 [hep-th].

[49] H. Casini, M. Huerta, and L. Leitao. "Entanglement entropy for a Dirac fermion in three dimensions: Vertex contribution". In: *Nucl. Phys.* B814 (2009), pp. 594–609. arXiv: 0811.1968 [hep-th].

[50] A. B. Zamolodchikov. "Irreversibility of the Flux of the Renormalization Group in a 2D Field Theory". In: *JETP Lett.* 43 (1986). [Pisma Zh. Eksp. Teor. Fiz.43,565(1986)], pp. 730–732.

[51] John L. Cardy. "Is There a c Theorem in Four-Dimensions?" In: *Phys. Lett.* B215 (1988), pp. 749–752.

[52] D. Anselmi et al. "Nonperturbative formulas for central functions of supersymmetric gauge theories". In: *Nucl. Phys.* B526 (1998), pp. 543–571. arXiv: hep-th/9708042 [hep-th].

[53] D. Anselmi et al. "Positivity constraints on anomalies in supersymmetric gauge theories". In: *Phys. Rev.* D57 (1998), pp. 7570–7588. arXiv: hep-th/9711035 [hep-th].

[54] Kenneth A. Intriligator and Brian Wecht. "The Exact superconformal R symmetry maximizes a". In: *Nucl. Phys.* B667 (2003), pp. 183–200. arXiv: hep-th/0304128 [hep-th].

[55] Edwin Barnes et al. "Evidence for the strongest version of the 4d a-theorem, via a-maximization along RG flows". In: *Nucl. Phys.* B702 (2004), pp. 131–162. arXiv: hep-th/0408156 [hep-th].

[56] Zohar Komargodski and Adam Schwimmer. "On Renormalization Group Flows in Four Dimensions". In: *JHEP* 12 (2011), p. 099. arXiv: 1107.3987 [hep-th].

[57] Daniel L. Jafferis et al. "Towards the F-Theorem: N=2 Field Theories on the Three-Sphere". In: *JHEP* 06 (2011), p. 102. arXiv: 1103.1181 [hep-th].

[58] Igor R. Klebanov, Silviu S. Pufu, and Benjamin R. Safdi. "F-Theorem without Supersymmetry". In: *JHEP* 10 (2011), p. 038. arXiv: 1105.4598 [hep-th].

[59] Antonio Amariti and Massimo Siani. "Z-extremization and F-theorem in Chern-Simons matter theories". In: *JHEP* 10 (2011), p. 016. arXiv: 1105.0933 [hep-th].

[60] Igor R. Klebanov et al. "Entanglement Entropy of 3-d Conformal Gauge Theories with Many Flavors". In: *JHEP* 05 (2012), p. 036. arXiv: 1112.5342 [hep-th].

[61] Igor R. Klebanov et al. "Renyi Entropies for Free Field Theories". In: *JHEP* 04 (2012), p. 074. arXiv: 1111.6290 [hep-th].

[62] J. S. Dowker. "Entanglement entropy for odd spheres". In: (2010). arXiv: 1012.1548 [hep-th].

[63] S. W. Hawking. "Particle Creation by Black Holes". In: *Commun. Math. Phys.* 43 (1975). [,167(1975)], pp. 199–220.

[64] S. S. Gubser, Igor R. Klebanov, and Alexander M. Polyakov. "Gauge theory correlators from noncritical string theory". In: *Phys. Lett.* B428 (1998), pp. 105–114. arXiv: hep-th/9802109 [hep-th].

[65] Edward Witten. "Anti-de Sitter space and holography". In: *Adv. Theor. Math. Phys.* 2 (1998), pp. 253–291. arXiv: hep-th/9802150 [hep-th].

[66] Ofer Aharony et al. "Large N field theories, string theory and gravity". In: *Phys. Rept.* 323 (2000), pp. 183–386. arXiv: hep-th/9905111 [hep-th].

[67] H. Casini and M. Huerta. "Entanglement entropy in free quantum field theory". In: *J. Phys.* A42 (2009), p. 504007. arXiv: 0905.2562 [hep-th].

[68] Pasquale Calabrese and John L. Cardy. "Entanglement entropy and quantum field theory". In: *J. Stat. Mech.* 0406 (2004), P06002. arXiv: hep-th/0405152 [hep-th].

[69] Shinsei Ryu and Tadashi Takayanagi. "Holographic derivation of entanglement entropy from AdS/CFT". In: *Phys. Rev. Lett.* 96 (2006), p. 181602. arXiv: hep-th/0603001 [hep-th].

[70] Eduardo Conde and Alfonso V. Ramallo. "On the gravity dual of Chern-Simons-matter theories with unquenched flavor". In: *JHEP* 07 (2011), p. 099. arXiv: 1105.6045 [hep-th].

[71] Niko Jokela et al. "Thermodynamics of the brane in Chern-Simons matter theories with flavor". In: *JHEP* 02 (2013), p. 144. arXiv: 1211.0630 [hep-th].

[72] Yago Bea et al. "Unquenched massive flavors and flows in Chern-Simons matter theories". In: *JHEP* 12 (2013), p. 033. arXiv: 1309.4453 [hep-th].

[73] Niko Jokela, Alfonso V. Ramallo, and Dimitrios Zoakos. "Magnetic catalysis in flavored ABJM". In: *JHEP* 02 (2014), p. 021. arXiv: 1311.6265 [hep-th].

[74] Yago Bea et al. "Flux and Hall states in ABJM with dynamical flavors". In: *JHEP* 03 (2015), p. 009. arXiv: 1411.3335 [hep-th].

[75] Leszek M. Sokołowski. "The bizarre anti-de Sitter spacetime". In: *Int. J. Geom. Meth. Mod. Phys.* 13.09 (2016), p. 1630016. arXiv: 1611.01118 [gr-qc].

[76] Carlos Alfonso Bayona and Nelson R. F. Braga. "Anti-de Sitter boundary in Poincare coordinates". In: *Gen. Rel. Grav.* 39 (2007), pp. 1367–1379. arXiv: hep-th/0512182 [hep-th].

[77] D. Christodoulou and Sergiù Klainerman. "The global nonlinear stability of the Minkowski space". In: *Séminaire Équations aux dérivées partielles (Polytechnique)* (1989-1990). talk:13.

[78] Helmut Friedrich. "On the existence of n-geodesically complete or future complete solutions of Einstein's field equations with smooth asymptotic structure". In: *Comm. Math. Phys.* 107.4 (1986), pp. 587–609.

[79] Piotr Bizon and Andrzej Rostworowski. "On weakly turbulent instability of anti-de Sitter space". In: *Phys. Rev. Lett.* 107 (2011), p. 031102. arXiv: 1104.3702 [gr-qc].

[80] Oscar J. C. Dias, Gary T. Horowitz, and Jorge E. Santos. "Gravitational Turbulent Instability of Anti-de Sitter Space". In: *Class. Quant. Grav.* 29 (2012), p. 194002. arXiv: 1109.1825 [hep-th].

[81] Oscar J. C. Dias et al. "On the Nonlinear Stability of Asymptotically Anti-de Sitter Solutions". In: *Class. Quant. Grav.* 29 (2012), p. 235019. arXiv: 1208.5772 [gr-qc].

[82] Alex Buchel, Luis Lehner, and Steven L. Liebling. "Scalar Collapse in AdS". In: *Phys. Rev.* D86 (2012), p. 123011. arXiv: 1210.0890 [gr-qc].

[83] Piotr Bizoń. "Is AdS stable?" In: *Gen. Rel. Grav.* 46.5 (2014), p. 1724. arXiv: 1312.5544 [gr-qc].

[84] Anxo Biasi, Javier Mas, and Alexandre Serantes. "Gravitational wave driving of a gapped holographic system". In: *JHEP* 05 (2019), p. 161. arXiv: 1903.05618 [hep-th].

[85] Pablo Carracedo et al. "Adiabatic pumping solutions in global AdS". In: *JHEP* 05 (2017), p. 141. arXiv: 1612.07701 [hep-th].

[86] Raúl Arias, Javier Mas, and Alexandre Serantes. "Stability of charged global AdS_4 spacetimes". In: *JHEP* 09 (2016), p. 024. arXiv: 1606.00830 [hep-th].

[87] Javier Abajo-Arrastia et al. "Holographic Relaxation of Finite Size Isolated Quantum Systems". In: *JHEP* 05 (2014), p. 126. arXiv: 1403.2632 [hep-th].

[88] Maciej Maliborski and Andrzej Rostworowski. "Time-Periodic Solutions in an Einstein AdS–Massless-Scalar-Field System". In: *Phys. Rev. Lett.* 111 (2013), p. 051102. arXiv: 1303.3186 [gr-qc].

[89] Venkat Balasubramanian et al. "Holographic Thermalization, Stability of Anti–de Sitter Space, and the Fermi-Pasta-Ulam Paradox". In: *Phys. Rev. Lett.* 113.7 (2014), p. 071601. arXiv: 1403.6471 [hep-th].

[90] Javier Mas and Alexandre Serantes. "Oscillating Shells in Anti-de Sitter Space". In: *Int. J. Mod. Phys.* D24.09 (2015), p. 1542003. arXiv: 1507.01533 [gr-qc].

[91] Emilia da Silva et al. "Collapse and Revival in Holographic Quenches". In: *JHEP* 04 (2015), p. 038. arXiv: 1412.6002 [hep-th].

[92] Fotios V. Dimitrakopoulos et al. "Position space analysis of the AdS (in)stability problem". In: *JHEP* 08 (2015), p. 077. arXiv: 1410.1880 [hep-th].

[93] Masanori Hanada, Goro Ishiki, and Hiromasa Watanabe. "Partial Deconfinement". In: *JHEP* 03 (2019), p. 145. arXiv: 1812.05494 [hep-th].

[94] Shinsei Ryu and Tadashi Takayanagi. "Aspects of Holographic Entanglement Entropy". In: *JHEP* 08 (2006), p. 045. arXiv: hep-th/0605073 [hep-th].

[95] Veronika E. Hubeny, Mukund Rangamani, and Tadashi Takayanagi. "A Covariant holographic entanglement entropy proposal". In: *JHEP* 07 (2007), p. 062. arXiv: 0705.0016 [hep-th].

[96] Matthew Headrick and Tadashi Takayanagi. "A Holographic proof of the strong subadditivity of entanglement entropy". In: *Phys. Rev.* D76 (2007), p. 106013. arXiv: 0704.3719 [hep-th].

[97] Patrick Hayden, Matthew Headrick, and Alexander Maloney. "Holographic Mutual Information is Monogamous". In: *Phys. Rev.* D87.4 (2013), p. 046003. arXiv: 1107.2940 [hep-th].

[98] Ning Bao et al. "The Holographic Entropy Cone". In: *JHEP* 09 (2015), p. 130. arXiv: 1505.07839 [hep-th].

[99] Jose L. F. Barbon and Carlos A. Fuertes. "Holographic entanglement entropy probes (non)locality". In: *JHEP* 04 (2008), p. 096. arXiv: 0803.1928 [hep-th].

[100] Willy Fischler, Arnab Kundu, and Sandipan Kundu. "Holographic Entanglement in a Noncommutative Gauge Theory". In: *JHEP* 01 (2014), p. 137. arXiv: 1307.2932 [hep-th].

[101] Joanna L. Karczmarek and Charles Rabideau. "Holographic entanglement entropy in nonlocal theories". In: *JHEP* 10 (2013), p. 078. arXiv: 1307.3517 [hep-th].

[102] Sergey N. Solodukhin. "Entanglement Entropy in Non-Relativistic Field Theories". In: *JHEP* 04 (2010), p. 101. arXiv: 0909.0277 [hep-th].

[103] Tomoyoshi Hirata and Tadashi Takayanagi. "AdS/CFT and strong subadditivity of entanglement entropy". In: *JHEP* 02 (2007), p. 042. arXiv: hep-th/0608213 [hep-th].

[104] Pablo Bueno and Robert C. Myers. "Universal entanglement for higher dimensional cones". In: *JHEP* 12 (2015), p. 168. arXiv: 1508.00587 [hep-th].

[105] Pablo Bueno, Robert C. Myers, and William Witczak-Krempa. "Universal corner entanglement from twist operators". In: *JHEP* 09 (2015), p. 091. arXiv: 1507.06997 [hep-th].

[106] Pablo Bueno, Robert C. Myers, and William Witczak-Krempa. "Universality of corner entanglement in conformal field theories". In: *Phys. Rev. Lett.* 115 (2015), p. 021602. arXiv: 1505.04804 [hep-th].

[107] Pablo Bueno and Robert C. Myers. "Corner contributions to holographic entanglement entropy". In: *JHEP* 08 (2015), p. 068. arXiv: 1505.07842 [hep-th].

[108] Thomas Faulkner, Aitor Lewkowycz, and Juan Maldacena. "Quantum corrections to holographic entanglement entropy". In: *JHEP* 11 (2013), p. 074. arXiv: 1307.2892 [hep-th].

[109] Taylor Barrella et al. "Holographic entanglement beyond classical gravity". In: *JHEP* 09 (2013), p. 109. arXiv: 1306.4682 [hep-th].

[110] Xi Dong. "Holographic Entanglement Entropy for General Higher Derivative Gravity". In: *JHEP* 01 (2014), p. 044. arXiv: 1310.5713 [hep-th].

[111] Joan Camps. "Generalized entropy and higher derivative Gravity". In: *JHEP* 03 (2014), p. 070. arXiv: 1310.6659 [hep-th].

[112] Aitor Lewkowycz and Juan Maldacena. "Generalized gravitational entropy". In: *JHEP* 08 (2013), p. 090. arXiv: 1304.4926 [hep-th].

[113] Xi Dong, Aitor Lewkowycz, and Mukund Rangamani. "Deriving covariant holographic entanglement". In: *JHEP* 11 (2016), p. 028. arXiv: 1607.07506 [hep-th].

[114] Dmitri V. Fursaev, Alexander Patrushev, and Sergey N. Solodukhin. "Distributional Geometry of Squashed Cones". In: *Phys. Rev.* D88.4 (2013), p. 044054. arXiv: 1306.4000 [hep-th].

[115] Kenneth A. Brakke. "The Surface Evolver". In: *Experimental Mathematics* 1.2 (1992), pp. 141–165.

[116] Piermarco Fonda et al. "On shape dependence of holographic mutual information in AdS_4". In: *JHEP* 02 (2015), p. 005. arXiv: 1411.3608 [hep-th].

[117] Bartlomiej Czech et al. "The Gravity Dual of a Density Matrix". In: *Class. Quant. Grav.* 29 (2012), p. 155009. arXiv: 1204.1330 [hep-th].

[118] Aron C. Wall. "Maximin Surfaces, and the Strong Subadditivity of the Covariant Holographic Entanglement Entropy". In: *Class. Quant. Grav.* 31.22 (2014), p. 225007. arXiv: 1211.3494 [hep-th].

[119] Matthew Headrick et al. "Causality & holographic entanglement entropy". In: *JHEP* 12 (2014), p. 162. arXiv: 1408.6300 [hep-th].

[120] Ben Freivogel et al. "Casting Shadows on Holographic Reconstruction". In: *Phys. Rev.* D91.8 (2015), p. 086013. arXiv: 1412.5175 [hep-th].

[121] Vijay Balasubramanian et al. "Entwinement and the emergence of spacetime". In: *JHEP* 01 (2015), p. 048. arXiv: 1406.5859 [hep-th].

[122] Vijay Balasubramanian et al. "Entanglement shadows in LLM geometries". In: *JHEP* 11 (2017), p. 159. arXiv: 1704.03448 [hep-th].

[123] John Hammersley. "Extracting the bulk metric from boundary information in asymptotically AdS spacetimes". In: *JHEP* 12 (2006), p. 047. arXiv: hep-th/0609202 [hep-th].

[124] John Hammersley. "Numerical metric extraction in AdS/CFT". In: *Gen. Rel. Grav.* 40 (2008), pp. 1619–1652. arXiv: 0705.0159 [hep-th].

[125] Samuel Bilson. "Extracting spacetimes using the AdS/CFT conjecture". In: *JHEP* 08 (2008), p. 073. arXiv: 0807.3695 [hep-th].

[126] Samuel Bilson. "Extracting Spacetimes using the AdS/CFT Conjecture: Part II". In: *JHEP* 02 (2011), p. 050. arXiv: 1012.1812 [hep-th].

[127] Michael Spillane. "Constructing Space From Entanglement Entropy". In: (2013). arXiv: 1311.4516 [hep-th].

[128] Ning Bao et al. "Towards Bulk Metric Reconstruction from Extremal Area Variations". In: (2019). arXiv: 1904.04834 [hep-th].

[129] Netta Engelhardt and Gary T. Horowitz. "Towards a Reconstruction of General Bulk Metrics". In: *Class. Quant. Grav.* 34.1 (2017), p. 015004. arXiv: 1605.01070 [hep-th].

[130] Brian Swingle. "Entanglement Renormalization and Holography". In: *Phys. Rev.* D86 (2012), p. 065007. arXiv: 0905.1317 [cond-mat.str-el].

[131] Brian Swingle. "Constructing holographic spacetimes using entanglement renormalization". In: (2012). arXiv: 1209.3304 [hep-th].

[132] Mark Van Raamsdonk. "Comments on quantum gravity and entanglement". In: (2009). arXiv: 0907.2939 [hep-th].

[133] Mark Van Raamsdonk. "Building up spacetime with quantum entanglement". In: *Gen. Rel. Grav.* 42 (2010). [Int. J. Mod. Phys.D19,2429(2010)], pp. 2323–2329. arXiv: 1005.3035 [hep-th].

[134] Mark Van Raamsdonk. "Building up spacetime with quantum entanglement II: It from BC-bit". In: (2018). arXiv: 1809.01197 [hep-th].

[135] Tom Banks et al. "AdS dynamics from conformal field theory". In: (1998). arXiv: hep-th/9808016 [hep-th].

[136] Alex Hamilton et al. "Holographic representation of local bulk operators". In: *Phys. Rev.* D74 (2006), p. 066009. arXiv: hep-th/0606141 [hep-th].

[137] Daniel Kabat, Gilad Lifschytz, and David A. Lowe. "Constructing local bulk observables in interacting AdS/CFT". In: *Phys. Rev.* D83 (2011), p. 106009. arXiv: 1102.2910 [hep-th].

[138] Daniel Kabat et al. "Holographic representation of bulk fields with spin in AdS/CFT". In: *Phys. Rev.* D86 (2012), p. 026004. arXiv: 1204.0126 [hep-th].

[139] Idse Heemskerk. "Construction of Bulk Fields with Gauge Redundancy". In: *JHEP* 09 (2012), p. 106. arXiv: 1201.3666 [hep-th].

[140] Ian A. Morrison. "Boundary-to-bulk maps for AdS causal wedges and the Reeh-Schlieder property in holography". In: *JHEP* 05 (2014), p. 053. arXiv: 1403.3426 [hep-th].

[141] Xi Dong, Daniel Harlow, and Aron C. Wall. "Reconstruction of Bulk Operators within the Entanglement Wedge in Gauge-Gravity Duality". In: *Phys. Rev. Lett.* 117.2 (2016), p. 021601. arXiv: 1601.05416 [hep-th].

[142] Ricardo Espíndola, Alberto Guijosa, and Juan F. Pedraza. "Entanglement Wedge Reconstruction and Entanglement of Purification". In: *Eur. Phys. J.* C78.8 (2018), p. 646. arXiv: 1804.05855 [hep-th].

[143] Vijay Balasubramanian et al. "Bulk curves from boundary data in holography". In: *Phys. Rev.* D89.8 (2014), p. 086004. arXiv: 1310.4204 [hep-th].

[144] Robert C. Myers, Junjie Rao, and Sotaro Sugishita. "Holographic Holes in Higher Dimensions". In: *JHEP* 06 (2014), p. 044. arXiv: 1403.3416 [hep-th].

[145] Matthew Headrick, Robert C. Myers, and Jason Wien. "Holographic Holes and Differential Entropy". In: *JHEP* 10 (2014), p. 149. arXiv: 1408.4770 [hep-th].

[146] Bartlomiej Czech, Xi Dong, and James Sully. "Holographic Reconstruction of General Bulk Surfaces". In: *JHEP* 11 (2014), p. 015. arXiv: 1406.4889 [hep-th].

[147] Thomas Faulkner et al. "Gravitation from Entanglement in Holographic CFTs". In: *JHEP* 03 (2014), p. 051. arXiv: 1312.7856 [hep-th].

[148] Bartlomiej Czech et al. "A Stereoscopic Look into the Bulk". In: *JHEP* 07 (2016), p. 129. arXiv: 1604.03110 [hep-th].

[149] Jan de Boer et al. "Entanglement, holography and causal diamonds". In: *JHEP* 08 (2016), p. 162. arXiv: 1606.03307 [hep-th].

[150] Michael M. Wolf et al. "Area Laws in Quantum Systems: Mutual Information and Correlations". In: *Phys. Rev. Lett.* 100.7 (2008), p. 070502. arXiv: 0704.3906 [quant-ph].

[151] Alfonso V. Ramallo. "Introduction to the AdS/CFT correspondence". In: *Springer Proc. Phys.* 161 (2015), pp. 411–474. arXiv: 1310.4319 [hep-th].

[152] Omer Ben-Ami, Dean Carmi, and Jacob Sonnenschein. "Holographic Entanglement Entropy of Multiple Strips". In: *JHEP* 11 (2014), p. 144. arXiv: 1409.6305 [hep-th].

[153] Tadashi Takayanagi and Koji Umemoto. "Entanglement of purification through holographic duality". In: *Nature Phys.* 14.6 (2018), pp. 573–577. arXiv: 1708.09393 [hep-th].

[154] Masamichi Miyaji and Tadashi Takayanagi. "Surface/State Correspondence as a Generalized Holography". In: *PTEP* 2015.7 (2015), 073B03. arXiv: 1503.03542 [hep-th].

[155] Masamichi Miyaji et al. "Continuous Multiscale Entanglement Renormalization Ansatz as Holographic Surface-State Correspondence". In: *Phys. Rev. Lett.* 115.17 (2015), p. 171602. arXiv: 1506.01353 [hep-th].

[156] Ning Bao, Aidan Chatwin-Davies, and Grant N. Remmen. "Entanglement of Purification and Multiboundary Wormhole Geometries". In: *JHEP* 02 (2019), p. 110. arXiv: 1811.01983 [hep-th].

[157] Ning Bao. "Minimal Purifications, Wormhole Geometries, and the Complexity=Action Proposal". In: (2018). arXiv: 1811.03113 [hep-th].

[158] Peng Liu et al. "Entanglement of Purification in Holographic Systems". In: (2019). arXiv: 1902.02243 [hep-th].